10.4 Equilibrium molecular dynamics

Equilibrium molecular dynamics (MD) simulates the evolution of a microscopic model of a material system in time in the absence of any thermodynamic driving forces that can lead to fluxes within the material. By invoking the ergodic hypothesis, one can calculate ensemble averaged structural and thermodynamic properties from a well-equilibrated MD simulation. In addition, by invoking linear response theory, one can obtain transport properties and in general characterize the dynamical response of the system to the imposition or removal of driving forces that keep the system away from thermodynamic equilibrium. In this latter respect, MD has an advantage over MC, which can only give equilibrium thermodynamic properties.

10.4.1 Formulations of the equations of motion

The mathematical description of the dynamics of a classical system evolving under the influence of interactions among its constituent particles was briefly discussed in Section 3.2.1. Several formulations of the differential equations describing a dynamical trajectory were mentioned there. We briefly review these formulations here.

Lagrangian formulation

Let q_k, $k = 1, 2, \ldots$ be the (independent) generalized coordinates used to describe the configuration of the system. These are collectively referred to as a vector $\mathbf{q}$. Let $\mathcal{V} = \mathcal{V}(\mathbf{q}, \dot{\mathbf{q}}, t)$ be the potential energy function and

$\mathcal{K} = \mathcal{K}(\mathbf{q}, \dot{\mathbf{q}}, t)$ be the kinetic energy function of the system.

We define the Lagrangian function as

$\mathcal{L} = \mathcal{L}(\mathbf{q}, \dot{\mathbf{q}}, t) \equiv \mathcal{K} - \mathcal{V}$

The trajectory $\mathbf{q}(t)$ satisfies the set of differential equations

$$\frac{d}{dt}\left(\frac{\partial \mathcal{L}}{\partial \dot{q}_k}\right) - \frac{\partial \mathcal{L}}{\partial q_k} = 0 \tag{10.57}$$

Eq. (10.57) is a differential expression of *Hamilton's variational principle* of least action: For a mechanical system in which all forces, except possible forces of constraint, are derivable from a generalized scalar potential $\mathcal{V}$ that may be a function of coordinates, velocities, and time, the motion of the system from time t_1 to time t_2 is such that the line integral

$$S_{cl} = \int_{t_1}^{t_2} \mathcal{L}(\mathbf{q}, \dot{\mathbf{q}}, t)\, dt$$

has a stationary point over the correct path of motion [Goldstein (1980)].

The momentum p_k conjugate to the generalized coordinate q_k is defined by

$$p_k = \frac{\partial \mathcal{L}(\mathbf{q}, \dot{\mathbf{q}}, t)}{\partial \dot{q}_k} \tag{3.1}$$

The Hamiltonian function $\mathcal{H}(\mathbf{q}, \mathbf{p}, t)$ is defined from the Lagrangian formulation as

$$\mathcal{H}(\mathbf{q}, \mathbf{p}, t) = \sum_k \dot{q}_k\, p_k - \mathcal{L}(\mathbf{q}, \dot{\mathbf{q}}, t) \tag{3.2}$$

If $\mathcal{L}$ does not depend explicitly on time, *i.e*, if it depends on time only through its dependence on $\mathbf{q}$ and $\dot{\mathbf{q}}$, then $\mathcal{H}$ is a constant of the motion, corresponding to the system total energy.

Hamiltonian formulation

In this formulation, one starts with the Hamiltonian function $\mathcal{H}(\mathbf{q}, \mathbf{p}, t)$. A differential description of the trajectory is given by the *canonical equations*

$$\dot{q}_k = \frac{\partial \mathcal{H}}{\partial p_k} \tag{3.5}$$

$$\dot{p}_k = -\frac{\partial \mathcal{H}}{\partial q_k} \tag{3.4}$$

If the Hamiltonian $\mathcal{H}$ does not depend explicitly on time, then, as one can readily prove from the canonical equations, $\mathcal{H}$ is a constant of the motion, corresponding to the total energy (*conservative* system).

Newtonian formulation

For a system whose configuration is described in terms of the cartesian coordinates $\mathbf{r}_i$ of constituent particles, a differential decription of the motion is given by the equations

$$m_i \ddot{\mathbf{r}} = \mathbf{F}_i \tag{10.58}$$

$$\mathbf{F}_i = -\nabla_{\mathbf{r}_i} \mathcal{V} \tag{10.59}$$

with m_i, $\mathbf{r}_i$, $\mathbf{F}_i$ the mass, coordinate vector, and total force acting on particle i, respectively, and $\mathcal{V}(\mathbf{r}_1, \ldots, \mathbf{r}_i, \ldots, \mathbf{r}_N)$ the potential energy function of the system.

In all of the above formulations, the coordinates $\mathbf{q}$ or $\mathbf{r}$ have been assumed independently variable. The equations have to be modified in the presence of *constraints* among the system degrees of freedom. The Lagrangian formulation reduces to a constrained

minimization of the action integral. In the Newtonian formulation, the presence of constraints among the site coordinates leads to an equation for the force $\mathbf{F}_i$ of the form

$$\mathbf{F}_i = -\nabla_{\mathbf{r}_i}\mathcal{V} + \mathbf{g}_i \tag{10.60}$$

where $\mathbf{g}_i$ the *constraint force* on site i. How the constraint forces $\mathbf{g}_i$ can be calculated, given the equations of constraint, is described below in our discussion of constraint dynamics algorithms (section 10.4.4).

In general, constraints on a dynamical system fall into one of two categories:

Holonomic constraints are cast in the form of *equations* involving only the coordinates $\mathbf{q}$ and time t. In other words, a holonomic constraint is of the form $f(\mathbf{q}, t) = 0$.

Nonholonomic constraints, on the other hand, are constraints that can only be expressed as inequalities, or involve time derivatives of the coordinates.

Figure 10.15 shows simple examples of a holonomic (a) and a nonholonomic (b) constraint. The circle of radius a in Fig. 10.15 (a) is constrained to roll without sliding on a line inclined by an angle α with respect to the x-axis. The configuration of the circle can be described in terms of the coordinates z and x of its center and the angle of rotation ϕ around its center. Clearly, since sliding is not possible, z, x, and ϕ are not independent, but have to always follow the equations

$$z = z_0 - a\,\phi\,\sin\alpha$$

$$x = x_0 - a\,\phi\,\cos\alpha$$

These are clearly of the form $f(x, z, \phi) = 0$, and therefore *holonomic* constraints. The circle of radius a in Figure 10.15 (b), on the other hand, is constrained to roll without sliding on the xy plane. (Think of a coin rolling on a table.) The plane of the circle is perpendicular to the xy plane at all times, but the angle θ between the vector normal to the circle plane and the x axis is free to change. The configuration of the system is described in terms of the generalized coordinates x, y, θ, and ϕ. (The z coordinate of the center is always a.) The condition of no sliding leads to the requirements

$$\dot{x} = -a \sin\theta \, \dot{\phi}$$

$$\dot{y} = -a \cos\theta \, \dot{\phi}$$

These are equations involving the *time derivatives* of x, y and ϕ, and θ itself. They are *nonholonomic* constraint equations. No holonomic constraint can be written for the coordinates x, y, θ, ϕ of this system.

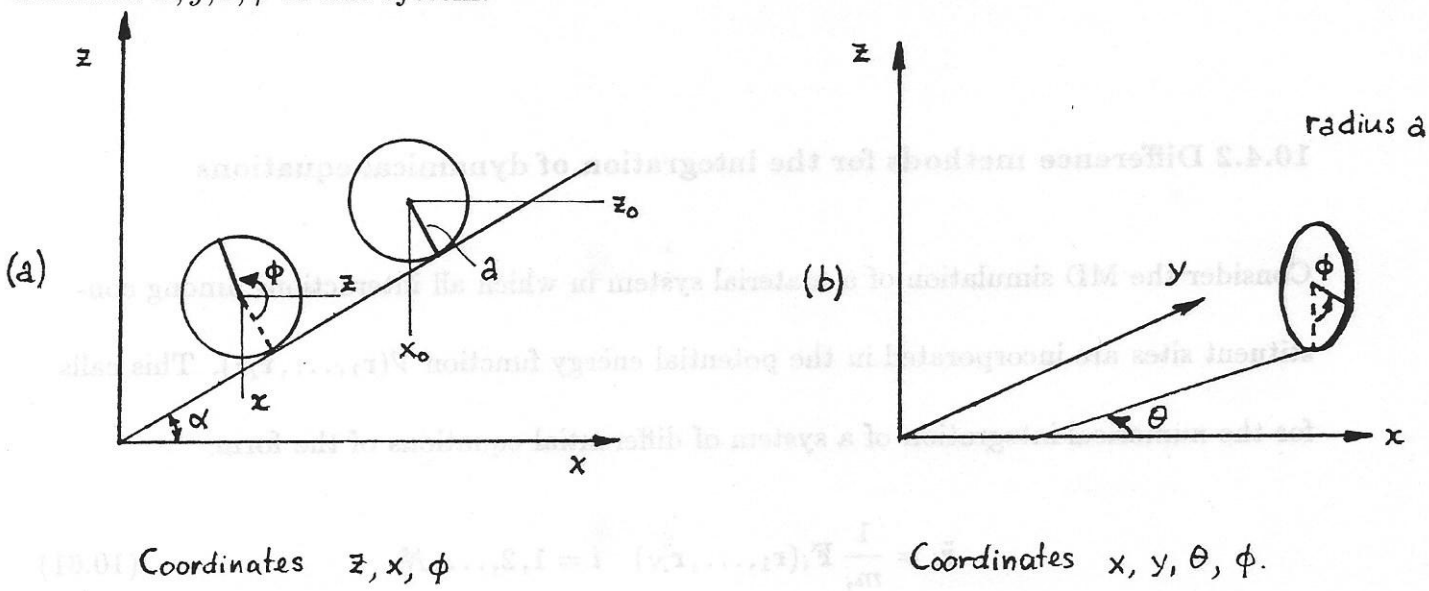

Figure 10.15 Examples of dynamical systems subject to constraints (a) holonomic; (b) nonholonomic.

In any formulation, the equations of motion are time-reversible. In an isolated system of interacting molecules, the quantities $\mathcal{H}$ (total energy), $\mathbf{P} = \sum_i \mathbf{p}_i$ (total linear momentum) and $\mathbf{L} = \sum_i \mathbf{r}_i \times \mathbf{p}_i$ (total angular momentum) are conserved. In a system of molecules confined to a box with periodic boundary conditions, on the other hand, which evolves in time subject only to interactions among the molecules and their images, $\mathcal{H}$ and $\mathbf{P}$ are conserved, but $\mathbf{L}$ is *not*. Every time a molecule crosses a face of the box and enters through the opposite face, a discontinuous change in the total angular momentun of the box is effected.

The most traditional type of MD simulation tracks such a system of molecules in a box with periodic boundary conditions; it is therefore carried out under conditions of constant N, V, E, and $\mathbf{P}$. It samples the phase-space probability distribution of the microcanonical ensemble, with the additional constraint that the total momentum is conserved.

10.4.2 Difference methods for the integration of dynamical equations

Consider the MD simulation of a material system in which all interactions among constituent sites are incorporated in the potential energy function $\mathcal{V}(\mathbf{r}_1, \ldots, \mathbf{r}_N)$. This calls for the numerical integration of a system of differential equations of the form

$$\ddot{\mathbf{r}}_i = \frac{1}{m_i} \mathbf{F}_i(\mathbf{r}_1, \ldots, \mathbf{r}_N) \quad i = 1, 2, \ldots, N \tag{10.61}$$

$$\mathbf{r}_i(0), \quad \dot{\mathbf{r}}_i(0) \quad \text{specified}$$

This is an *initial value problem.* It can be converted to a system of coupled first-order ordinary differential equations by the substitution:

$$\mathbf{r}_i = \mathbf{v}_i$$

$$\dot{\mathbf{v}}_i = \frac{1}{m_i}\mathbf{F}_i(\mathbf{r}_1, \mathbf{r}_2, \ldots, \mathbf{r}_N) \quad i = 1, 2, \ldots, N$$

$$\mathbf{r}_i(0),\ \mathbf{v}_i(0) \ \text{ specified}$$

With $\mathbf{y} \equiv \begin{bmatrix} \mathbf{r} \\ \mathbf{v} \end{bmatrix}$, this system is of the general form

$$\dot{\mathbf{y}} = \mathbf{f}(t, \mathbf{y}) \tag{10.62}$$

$$\mathbf{y}(0) \ \text{ specified}$$

As we know from initial value problems in chemical engineering, a variety of *difference methods* are availabe for solving the differential system of Eq. (10.62) [see Press *et al.* (1986)]. Generally, one marches along the independent variable (time) in finite steps δt. The step size may either be constant or changed *adaptively* during the numerical solution. The numerical scheme for the determination of $\mathbf{y}(t)$ is called n^{th} *order* when the error

$$\epsilon = ||\mathbf{y}^{numerical}(t) - \mathbf{y}^{exact}(t)|| = \mathcal{O}\left[(\delta t)^{n+1}\right]$$

In choosing an algorithm for the integration of the equations (10.62), one must give consideration to some factors that distinguish MD from other initial value problems, such as the following:

- The most time consuming part of an MD computation is the evaluation of forces on sites. Thus, a good criterion for the efficiency of a MD algorithm is that the ratio

$$\frac{\text{Number of } \mathbf{f} - \text{evaluations}}{\text{simulated time}} = \text{minimal} \tag{10.63}$$

The speed of all other computations involved in the algorithm is immaterial, as the whole calculation is dominated by the f-evaluation. From Eq. (10.63), it is apparent that the algorithm must not require many f-evaluations per integration time step. Otherwise popular schemes, such as the 4^{th} order Runge- Kutta-Gill method, are seldom used in MD because they do not fulfil this criterion. Again from Eq. (10.63), the algorithm must allow employing a long integration time step δt. There is, of course, a compromise between the number of function evaluations and the magnitude of the time step that can be used.

- The algorithm must be *stable*. This means that the error ϵ must not increase rapidly with increasing δt. The stability problem is severe in *stiff* systems of ODE's, possessing two or more widely disparate characteristic time scales. MD simulations of molecular systems are typically stiff, because of the wide spectrum of frequencies or characteristic times governing bond vibrational, torsional, translational, and long-range collective motions. Generally, stiffness in initial value problems can be alleviated by the use of implicit algorithms. Such algorithms are not favored in MD, however, as they require many f- evaluations.
- The integration algorithm should require little memory.
- The algorithm must be *accurate*; this means that the error ϵ, defined above, must be small for reasonably large δt. With regard to an algorithm's ability to describe the

"exact" dynamical trajectory, one can say the following: MD problems, being highly nonlinear, are characterized by tremendous sensitivity to initial conditions; any two trajectories that are initially very close will eventually diverge from each other exponentially with elapsed time. Clearly, there is no hope of tracking the "real" trajectory at long times. This is not a problem for extracting meaningful dynamical information from the MD run, provided the MD trajectory stays close to the "real" trajectory over the correlation times of interest. It is also not a problem as regards accumulating thermodynamic averages; for example, as long as the energy is conserved within narrow limits, the MD trajectory provides correct sampling of the NVE ensemble.

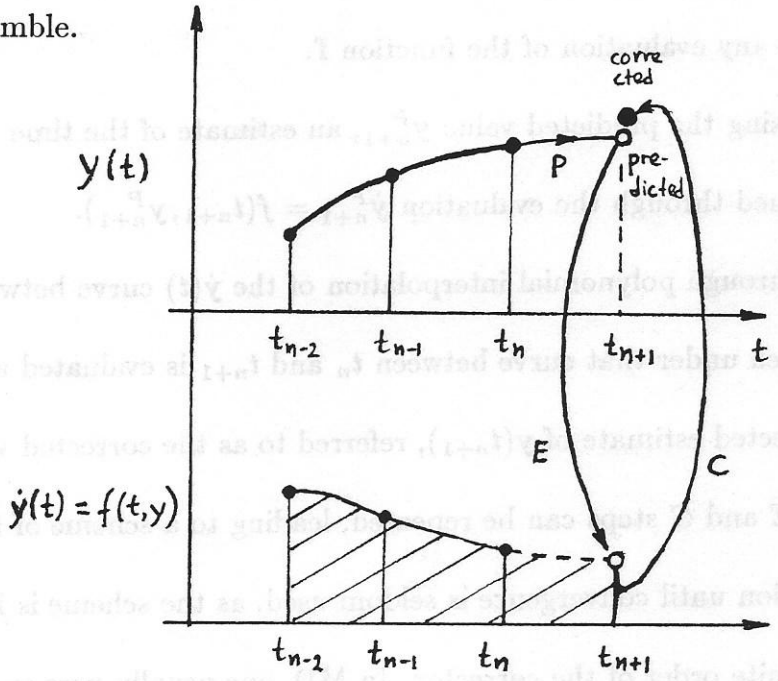

Figure 10.16 Schematic of a $k = 4$-value, $\ell = 3$-step predictor- corrector algorithm.

Gear Predictor-Corrector methods [Gear (1971)]. These methods for solving the initial value problem, Eq. (10.62), are widely used in MD. For a general discussion

see Press *et al.* (1986). The basic idea in a predictor-corrector algorithm is graphically outlined in Figure 10.16.

Assume that the integration has been performed up to time t_n. Estimates of the unknown function $\mathbf{y}$ and its time derivative $\dot{\mathbf{y}}(t) = \mathbf{f}(t, \mathbf{y})$ are available at all node points along the time axis, $t_i, i \leq n$. Calculations over the time interval t_n to t_{n+1} proceed as follows:

P (*Prediction*): Information about $\mathbf{y}$ and its derivatives, accumulated over steps $n-\ell+1$ to n, is extrapolated to obtain an estimate of $\mathbf{y}(t_{n+1})$, referred to as the predicted value $\mathbf{y}^P_{n+1}$. This prediction rests essentially on a Taylor expansion around t_n, and does not involve any evaluation of the function $\mathbf{f}$.

E (*Evaluation*): Using the predicted value $\mathbf{y}^P_{n+1}$, an estimate of the time derivative $\dot{\mathbf{y}}(t_{n+1})$ is obtained through the evaluation $\dot{\mathbf{y}}^P_{n+1} = f(t_{n+1}, \mathbf{y}^P_{n+1})$.

C (*Correction*): Through polynomial interpolation of the $\dot{\mathbf{y}}(t)$ curve between $t_{n-\ell+1}$ and t_{n+1}, the area under that curve between t_n and t_{n+1} is evaluated and used to obtain a corrected estimate of $\mathbf{y}(t_{n+1})$, referred to as the corrected value $\mathbf{y}^c_{n+1}$. In general, the E and C steps can be repeated, leading to a scheme of the form $P(EC)^m$. Iteration until convergence is seldom used, as the scheme is intrinsically limited by the finite order of the corrector. In MD, one usually uses $m = 1$ to avoid many expensive function evaluations.

In general, a $k - value$ predictor-corrector method uses k previously calculated values of $\mathbf{y}$ or its derivatives, while an $\ell - step$ method uses values calculated at ℓ previous

mesh points along the t axis. A $k-value$ method can be formulated in one of two equivalent representations. In the *Adams-Bashforth-Moulton* representation ($\ell = k-1$), one stores and updates the vector

$$(\mathbf{y}_n, \delta t\,\dot{\mathbf{y}}_n, \delta t\,\dot{\mathbf{y}}_{n-1}, \ldots, \delta t\,\dot{\mathbf{y}}_{n-k+2})$$

(compare Figure 10.16). In the *Nordsieck* representation, one stores and updates the values

$$\left(\mathbf{y}_n, \delta t\,\dot{\mathbf{y}}_n, \frac{\delta t^2}{2}\ddot{\mathbf{y}}_n, \ldots, \delta t^{k-1}\frac{\mathbf{y}_n^{(k-1)}}{(k-1)!}\right)$$

The equivalence between the Adams-Bashforth-Moulton and Nordsieck representations is discussed by van Gunsteren and Berendsen (1977).

As an example, we present here a four-value Gear predictor-corrector algorithm in the Nordsieck representation that is convenient for integrating the system of Newtonian equations of motion

$$\ddot{\mathbf{r}} = \mathbf{f}(\mathbf{r}) \tag{10.64}$$

Let

$$\begin{bmatrix} \mathbf{r}_0(t) \\ \mathbf{r}_1(t) \\ \mathbf{r}_2(t) \\ \mathbf{r}_3(t) \end{bmatrix} \equiv \begin{bmatrix} \mathbf{r}(t) \\ \delta t\,\dot{\mathbf{r}}(t) \\ \delta t^2/2\,\ddot{\mathbf{r}}(t) \\ \delta t^3/6\,\dddot{\mathbf{r}}(t) \end{bmatrix}$$

The predictor scheme is

$$\begin{bmatrix} \mathbf{r}_0^P(t+\delta t) \\ \mathbf{r}_1^P(t+\delta t) \\ \mathbf{r}_2^P(t+\delta t) \\ \mathbf{r}_3^P(t+\delta t) \end{bmatrix} = \begin{bmatrix} 1 & 1 & 1 & 1 \\ 0 & 1 & 2 & 3 \\ 0 & 0 & 1 & 3 \\ 0 & 0 & 0 & 1 \end{bmatrix} \begin{bmatrix} \mathbf{r}_0^P(t) \\ \mathbf{r}_1^P(t) \\ \mathbf{r}_2^P(t) \\ \mathbf{r}_3^P(t) \end{bmatrix} \tag{10.65}$$

Eq. (10.65) is a set of Taylor series expansions for the positions, velocities, accelerations, and third temporal derivatives of the positions. The matrix appearing in it is known as Pascal triangle matrix. The corrector scheme is

$$\begin{bmatrix} \mathbf{r}_0^C(t+\delta t) \\ \mathbf{r}_1^C(t+\delta t) \\ \mathbf{r}_2^C(t+\delta t) \\ \mathbf{r}_3^C(t+\delta t) \end{bmatrix} = \begin{bmatrix} \mathbf{r}_0^P(t+\delta t) \\ \mathbf{r}_1^P(t+\delta t) \\ \mathbf{r}_2^P(t+\delta t) \\ \mathbf{r}_3^P(t+\delta t) \end{bmatrix} + \begin{bmatrix} 1/6 \\ 5/6 \\ 1 \\ 1/3 \end{bmatrix} \left(\frac{\delta t^2}{2} \mathbf{f}(\mathbf{r}_0^P) - \mathbf{r}_2^P \right) \tag{10.66}$$

The correction clearly depends on the difference between the predicted accelerations $\mathbf{r}_2^P$ and the accelerations evaluated from the predicted positions. The coefficients of the corrector have been calculated for optimal stability and accuracy. For a system with a total of N coordinates ($N/3$ atoms), the four-value Gear algorithm requires $5N$ words of storage. Analogous schemes are available for differential systems of the form $\dot{\mathbf{r}} = \mathbf{f}(\mathbf{r})$ and $\ddot{\mathbf{r}} = \mathbf{f}(\mathbf{r}, \dot{\mathbf{r}})$. ~~Analogous schemes for differential systems of the form~~

The Verlet Algorithms

This family of algorithms are simple, accurate, easy to program, economical in storage, and therefore quite popular. The original Verlet scheme can be thought of as a 3-value, 2-step predictor-corrector method, where the predictor and corrector steps coincide (no corrector step is needed).

Verlet's original method (1967) for the problem

$$\ddot{\mathbf{r}} = \mathbf{f}(\mathbf{r}) \equiv \mathbf{a}(\mathbf{r})$$

calculates the positions at $t + \delta t$ from the positions at t, the positions at $t - \delta t$, and the accelerations at t by

$$\mathbf{r}(t + \delta t) = 2\,\mathbf{r}(t) - \mathbf{r}(t - \delta t) + \delta t^2\,\mathbf{a}(t) + \mathcal{O}(\delta t^4) \tag{10.67}$$

Eq. (10.67) is a consequence of adding the two Taylor expansions

$$\mathbf{r}(t + \delta t) = \mathbf{r}(t) + \delta t\,\mathbf{v}(t) + \frac{1}{2}\delta t^2\,\mathbf{a}(t) + \frac{1}{6}\delta t^3\,\mathbf{b}(t) + \cdots$$

$$\mathbf{r}(t - \delta t) = \mathbf{r}(t) - \delta t\,\mathbf{v}(t) + \frac{1}{2}\delta t^2\,\mathbf{a}(t) - \frac{1}{6}\delta t^3\,\mathbf{b}(t) + \cdots$$

The velocities can be estimated by

$$\mathbf{v}(t) = \frac{\mathbf{r}(t + \delta t) - \mathbf{r}(t - \delta t)}{2\,\delta t} + \mathcal{O}(\delta t^2) \tag{10.68}$$

Note that the velocity estimation scheme is of inferior order relative to the position estimation scheme. The Verlet algorithm requires only $3N$ words of storage, with N the total number of coordinates in the system. It is time reversible by construction and provides excellent energy conservation. For example, in an NVE MD simulation of liquid argon with time step $\delta t = 10^{-14}$s, energy fluctuations do not exceed $10^{-4}\epsilon$ over a typical run. When the time step is increased to $\delta t = 4 \times 10^{-14}$s, the energy fluctuations become $2 \times 10^{-3}\epsilon$. The sequence of calculations in a step of the Verlet algorithm is shown in Figure 10.17(a).

The Verlet "leap frog" algorithm [Hockney (1970)]

Verlet's original scheme, Eq. (10.67), generates the trajectory by adding a small ($\mathcal{O}(\delta t^2)$) term to the difference between two large ($\mathcal{O}(\delta t^0)$) terms; this may introduce

numerical imprecision. This problem is corrected in the Verlet "leap frog" scheme, which proceeds as follows:

$$\mathbf{r}(t+\delta t) = \mathbf{r}(t) + \delta t\, \mathbf{v}(t+1/2\delta t) \tag{10.69}$$

$$\mathbf{v}(t+1/2\delta t) = \mathbf{v}(t-1/2\delta t) + \delta t\, \mathbf{a}(t) \tag{10.70}$$

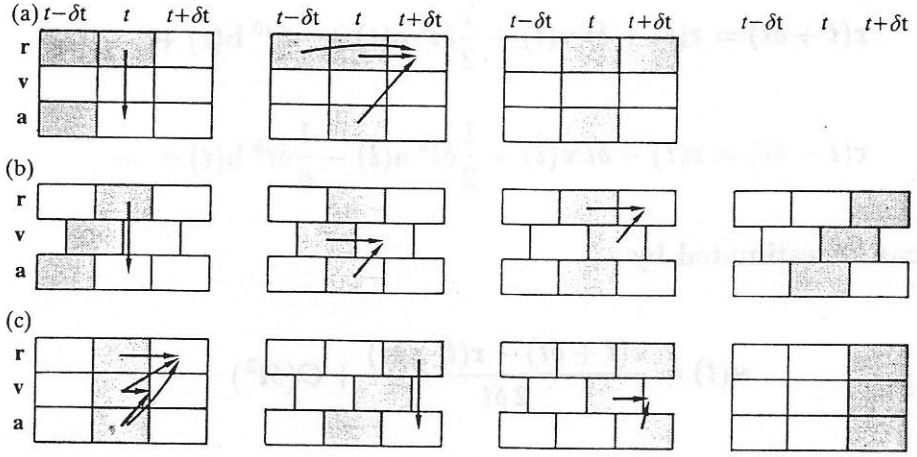

Figure 10.17 Sequence of calculations in a step of the Verlet algorithm. (*a*) Verlet's original method; (*b*) The leap-frog method; (*c*) Velocity Verlet algorithm. The stored variables are shown in grey boxes [after Allen and Tildesley (1986)].

The calculation of positions uses mid-step velocities. If velocities at integer time steps are needed, they can be calculated by

$$\mathbf{v}(t) = \frac{1}{2}\left[\mathbf{v}(t+1/2\delta t) + \mathbf{v}(t-1/2\delta t)\right] \tag{10.71}$$

The leap-frog method is algebraically equivalent to the original Verlet algorithm. The required storage is $3N$ words, which can be compressed to $2N$ by sacrificing Eq. (10.71).

Calculations involved in one step of trajectory generation are shown schematically in Figure 10.17(b).

The "velocity Verlet" algorithm [Swope et al. (1982)]

This algorithm is widely viewed as the most attractive variant of the Verlet method proposed to date. It proceeds by using the following equations:

$$\mathbf{r}(t+\delta t) = \mathbf{r}(t) + \delta t\,\mathbf{v}(t) + \frac{1}{2}\delta t^2\,\mathbf{a}(t) \tag{10.72}$$

$$\mathbf{v}(t+\frac{1}{2}\delta t) = \mathbf{v}(t) + \frac{1}{2}\delta t\,\mathbf{a}(t) \tag{10.73}$$

$$\mathbf{v}(t+\delta t) = \mathbf{v}(t+\frac{1}{2}\delta t) + \frac{1}{2}\delta t\,\mathbf{a}(t+\delta t) \tag{10.74}$$

$3N$ words of storage are required. The calculations involved in one step of the algorithm are shown in Figure 10.17(c).

10.4.3 MD of rigid, nonlinear polyatomic molecules in generalized coordinates

In this section we consider technical aspects of performing MD simulations of fluids consisting of small nonlinear polyatomic molecules with no torsional degrees of freedom, such as water, ammonia, benzene, methane *etc.* We use this discussion as a starting point for reviewing ways of describing the dynamics of rigid body motion. If potential expressions are employed to describe the energetic consequences of distortions of bonds and bond angles in each molecule, the molecular system can be treated as a collection of sites subject to bonded and nonbonded forces, and its motion can be tracked though the algorithms described above (*e.g.*, predictor-corrector, Verlet). One problem with this

approach is that it results in a stiff differential system; an extremely small time step is required for tracking the fast bond vibrations. On the other hand, a classical treatment for high-energy vibrational motions, especially motions involving light atoms, such as hydrogen, is not justifiable (see Section 4.6). For these reasons, it is physically reasonable and computationally economical to fix bond lengths and bond angles at their equilibrium values. One should note that fixing bond angles is less reasonable for molecules with internal torsional degrees of freedom, as it prevents cooperativity between bond angle vibrational and torsional motion amd may artificially slow down the dynamics of conformational isomerization. Fixing bond lengths and/or bond angles amounts to introducing *holonomic constraints* among the cartesian coordinates of sites. For example, fixing the bond length between two sites, 1 and 2, introduces the constraint

$$|\mathbf{r}_1 - \mathbf{r}_2|^2 = d_{12}^2$$

In the presence of constraints, cartesian coordinates are no longer independent. If one formulates the dynamics in cartesian coordinates, one has to introduce constraint forces [see Eq. (10.60) and following discussion]. The magnitude of a constraint force is in essence a Lagrange multiplier associated with the constraint that generates it. This method of integrating the equations of motion in cartesian coordinates in the presence of constraints is discussed in Section 10.4.4.

Alternatively, one can choose to describe each molecule in terms of a set of independent *generalized coordinates* and formulate the dynamics in terms of these coordinates

(see Section 4.6). It is this approach that we wish to examine in this section. The configuration of a nonlinear rigid polyatomic molecule is fully specified by 6 degrees of freedom:

$$\mathbf{r}_{CM}, \quad \Phi, \Theta, \Psi$$

$\mathbf{r}_{CM}$ is the position vector of the molecular center of mass. Φ, Θ, and Ψ are the Eulerian angles, specifying the overall orientation of the molecule with respect to the laboratory frame of reference.

For the definition of Eulerian angles it is useful to consider a frame of reference, b, that is permanently fixed to the molecule and rigidly rotating with it. A convenient choice for b is the frame formed by the three principal axes of the molecule. Let s stand for the "laboratory" frame of reference that is fixed in space. A schematic of b and s in the case of a water molecule is given in Figure 10.18.

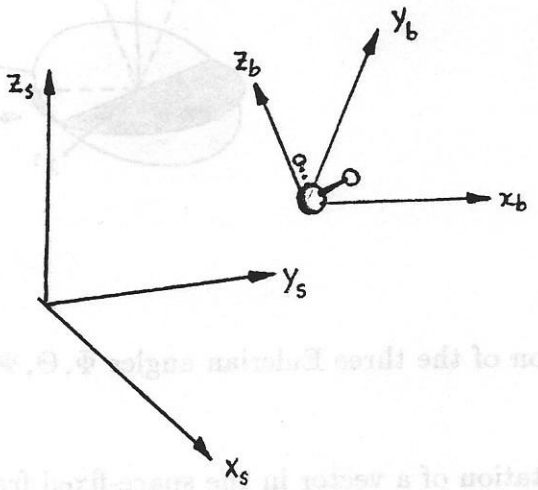

Figure 10.18 Schematic of laboratory frame, s, and body-fixed frame, b, used in describing the motion of a water molecule. b is chosen as the principal axis system of the water molecule.

The Eulerian angles specify the relative orientation of frames s and b. One common way of defining them [Goldstein (1980)] considers three rotation transformations whereby s can be brought onto b, as shown in Figure 10.19. The s-frame is first rotated around the z_s axis by an angle Φ, such that the rotated axis x' is directed along the line of intersection of planes $x_s\, y_s$ and $x_b\, y_b$. Next, the transformed system $x'\, y'\, z_s$ is rotated around the x' axis by Θ, until the new location z'' of the z axis coincides with z_b. Finally, the system $x'\, y''\, z_b$ is rotated around the z_b axis by an angle Ψ, until the axes x' and y'' come to x_b and y_b, respectively.

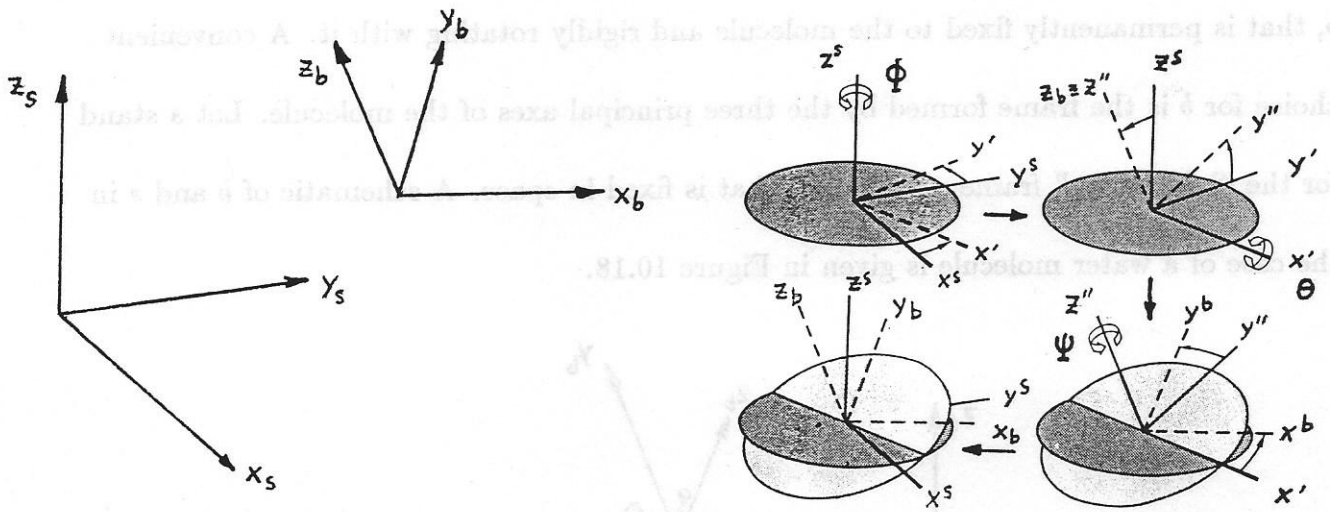

Figure 10.19 Definition of the three Eulerian angles Φ, Θ, Ψ.

Let $\mathbf{v}^s$ be the representation of a vector in the space-fixed frame s and $\mathbf{v}^b$ is the representation of the same vector in the body-fixed system b. The two representations are related by

$$\mathbf{v}^b = \mathbf{A}\, \mathbf{v}^s \tag{10.73}$$

where $\mathbf{A}$ a coordinate transformation matrix related to Φ, Θ, and Ψ as

$$\mathbf{A} = \begin{bmatrix} \cos\Psi & \sin\Psi & 0 \\ -\sin\Psi & \cos\Psi & 0 \\ 0 & 0 & 1 \end{bmatrix} \begin{bmatrix} 1 & 0 & 1 \\ 0 & \cos\Theta & 0 \\ 0 & -\sin\Theta & \cos\Theta \end{bmatrix} \begin{bmatrix} \cos\Phi & \sin\Phi & 0 \\ -\sin\Phi & \cos\Phi & 0 \\ 0 & 0 & 1 \end{bmatrix} =$$

$$\begin{bmatrix} \cos\Phi\cos\Psi - \sin\Phi\cos\Theta\sin\Psi & \sin\Phi\cos\Psi + \cos\Phi\cos\Theta\sin\Psi & \sin\Theta\sin\Psi \\ -\cos\Phi\sin\Psi - \sin\Phi\cos\Theta\cos\Psi & -\sin\Phi\sin\Psi + \cos\Phi\cos\Theta\cos\Psi & \sin\Theta\cos\Psi \\ \sin\Phi\sin\Theta & -\cos\Phi\sin\Theta & \cos\Theta \end{bmatrix} \tag{10.74}$$

As expected from Figure 10.19, $\mathbf{A}$ is the product of three rotation matrices. It is orthogonal ($\mathbf{A}^{-1} = \mathbf{A}^T$), which ensures that the transformation between s and b frames is metric preserving.

In any coordinate frame, the dynamics of rigid body motion can be described in terms of (a) three equations describing the translation of the center of mass under the influence of the total force

$$\mathbf{F} = \sum_{\alpha} \mathbf{F}_{\alpha} \tag{10.75}$$

where α labels the interaction sites constituting the molecule and $\mathbf{F}_{\alpha}$ stands for the external total force on site α; (b) three equations describing rotation around the center of mass under the influence of the total torque on the molecule,

$$\mathcal{T} = \sum_{\alpha} (\mathbf{r}_{\alpha} - \mathbf{r}_{CM}) \times \mathbf{F}_{\alpha} \equiv \sum_{\alpha} \mathbf{r}'_{\alpha} \times \mathbf{F}_{\alpha} \tag{10.76}$$

where we have introduced the notation $\mathbf{r}'_{\alpha}$ for the vector connecting the position of site α with the center of mass of the molecule. The translational motion of the center of mass is described by Newton's second law of motion

$$\mathbf{F} = \dot{\mathbf{p}}_{CM} \tag{10.77}$$

For the description of the rotational motion around the center of mass it is useful to define the angular momentum, **L**, as

$$\mathbf{L} = \sum_{\alpha} m_\alpha \, \mathbf{r}'_\alpha \times \dot{\mathbf{r}}'_\alpha \tag{10.78}$$

L is related to the angular velocity ω by

$$\mathbf{L} = \mathbf{I} \cdot \omega \tag{10.79}$$

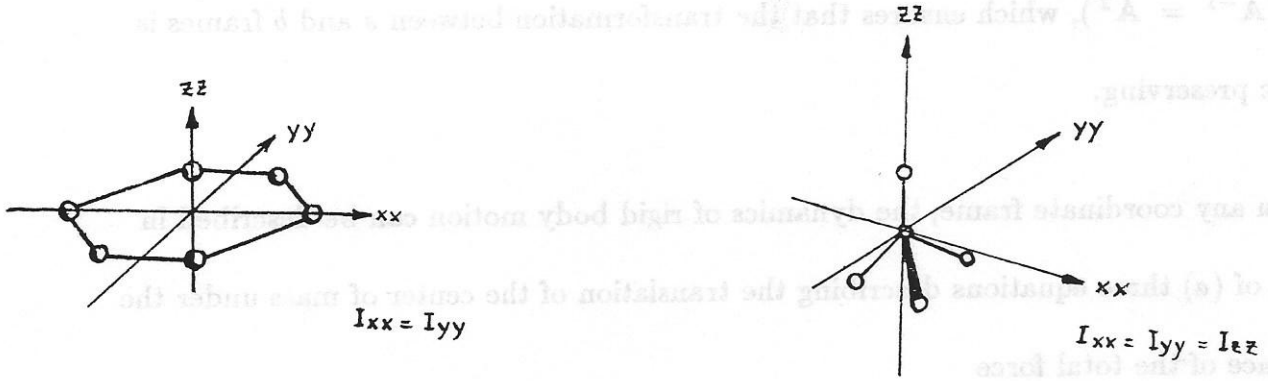

Figure 10.20 Examples of a molecule with cylindrical symmetry (united atom benzene) and a molecule with spherical symmetry (methane). A set of principal axes is shown for each molecule. In the case of benzene, the zz axis is uniquely defined but xx and zz are degenerate. In the case of methane, all principal axes are degenerate; the moment of inertia tensor is diagonal with respect to any set of orthogonal axes passing through the center of mass, with all three diagonal elements being equal.

In Eq. (10.79), **I** is the *moment of inertia tensor*, defined as

$$\mathbf{I} \equiv \sum_{\alpha} m_\alpha \left(r'^{\,2}_\alpha \mathbf{1} - \mathbf{r}'_\alpha \mathbf{r}'_\alpha \right) = \sum_{\alpha} m_\alpha \begin{bmatrix} y'^{\,2}_\alpha + z'^{\,2}_\alpha & r'^{\,2}_\alpha - x'_\alpha y'_\alpha & r'^{\,2}_\alpha - x'_\alpha z'_\alpha \\ r'^{\,2}_\alpha - y'_\alpha x'_\alpha & z'^{\,2}_\alpha + x'^{\,2}_\alpha & r'^{\,2}_\alpha - y'_\alpha z'_\alpha \\ r'^{\,2}_\alpha - z'_\alpha x'_\alpha & r'^{\,2}_\alpha - z'_\alpha y'_\alpha & x'^{\,2}_\alpha + y'^{\,2}_\alpha \end{bmatrix} \tag{10.80}$$

careful!

where $\mathbf{1}$ stands for the unit tensor of second order. Diagonalization of $\mathbf{I}$ yields the principal moments of inertia I_{xx}, I_{yy}, I_{zz} as eigenvalues, while the corresponding eigenvectors are the principal axes of the molecule. For a molecule with cylindrical symmetry, two principal moments of inertia are equal. For a molecule with spherical symmetry, all three principal moments of inertia are equal (see Figure 10.20)

The dynamical equations describing rigid rotation around the center of mass are of the form

$$\mathcal{T} = \dot{\mathbf{L}} \tag{10.81}$$

Note the analogy between Eq. (10.81) and Eq. (10.77) for translational motion. In a body-fixed coordinate system b that coincides with the principal axis system, the combination of Eqs. (10.78) and (10.81) leads to a particularly simple form:

$$\mathcal{T}^b = \mathbf{I}^b \cdot \dot{\omega}^b + \omega^b \times \left(\mathbf{I}^b \cdot \omega^b\right) \tag{10.82}$$

with

$$\mathbf{I}^b = \begin{bmatrix} I_{xx} & 0 & 0 \\ 0 & I_{yy} & 0 \\ 0 & 0 & I_{zz} \end{bmatrix}$$

the diagonal representation of the moment of inertia tensor in the principal axis system. Eqs. (10.82) are known as the *Euler equations*. The Euler equations permit a determination of the angular accelerations in the principal axis system from the torque, the angular velocities, and the moments of inertia in that system.

The following is a complete formulation of the dynamical equations of rotational motion in the generalized coordinates Ψ, Θ, Φ:

$$\mathcal{T}^s = \sum_\alpha (\mathbf{r}^s_\alpha - \mathbf{r}^s_{CM}) \times \mathbf{F}^s_\alpha \tag{10.83}$$

$$\mathcal{T}^b = \mathbf{A}\,\mathcal{T}^s \tag{10.84}$$

$$\dot{\omega}^b_x = \frac{\mathcal{T}^b_x}{I_{xx}} + \frac{I_{yy} - I_{zz}}{I_{xx}}\,\omega^b_y\,\omega^b_z \tag{10.85a}$$

$$\dot{\omega}^b_y = \frac{\mathcal{T}^b_y}{I_{yy}} + \frac{I_{zz} - I_{xx}}{I_{yy}}\,\omega^b_z\,\omega^b_x \tag{10.85b}$$

$$\dot{\omega}^b_z = \frac{\mathcal{T}^b_z}{I_{zz}} + \frac{I_{xx} - I_{yy}}{I_{zz}}\,\omega^b_x\,\omega^b_y \tag{10.85c}$$

$$\omega^s = \mathbf{A}^\top \omega^b \tag{10.86}$$

$$\dot{\Phi} = -\omega^s_x \frac{\sin\Phi\,\cos\Theta}{\sin\Theta} + \omega^s_y \frac{\cos\Phi\,\cos\Theta}{\sin\Theta} + \omega^s_z \tag{10.87a}$$

$$\dot{\Theta} = \omega^s_x \cos\Phi + \omega^s_y \sin\Phi \tag{10.87b}$$

$$\dot{\Psi} = \omega^s_x \frac{\sin\Phi}{\sin\Theta} - \omega^s_y \frac{\cos\Phi}{\sin\Theta} \tag{10.87c}$$

where the transformation matrix $\mathbf{A}$ is given in terms of Φ, Θ, and Ψ by Eq. (10.74). The coordinates of the sites in the laboratory frame s can be obtained from the (fixed) coordinates in the b frame by

$$\mathbf{r}_\alpha^s - \mathbf{r}_\beta^s = \mathbf{A}^T \left(\mathbf{r}_\alpha^b - \mathbf{r}_\beta^b \right) \quad \text{for every } \alpha, \beta \tag{10.88}$$

The system of equations (10.83) to (10.88) can be solved numerically as an initial value problem. In Eq. (10.83), the components of the torque are calculated in the laboratory frame from the current configuration. Eq. (10.84) gives the components of the torque vector in the body-fixed frame. Eqs. (10.85) are the Euler equations (10.82) in a slightly different form. By integrating these equations over a small time step δt, one obtains the angular velocities in the body-fixed frame at the end of the time step. The updated angular velocities in the laboratory frame are obtained through the coordinate transformation, Eq. (10.86). Eqs. (10.87) stem from the definition of the Eulerian angles. They permit calculating the Eulerian angles at the end of the time step from the angular velocities in the laboratory frame. Finally, the new site coordinates in the laboratory frame are updated via Eq. (10.88).

A drawback of the system of equations, Eq. (10.83) to (10.88), is that it calls for repeated coordinate transformations between the laboratory frame and the principal axis frame for each molecule. A more significant drawback is that $\dot{\Phi}$ amd $\dot{\Psi}$, as calculated from Eqs. (10.87), diverge whenever $\sin\Theta \to 0$; as seen from Figure 10.19, in the limit $\Theta \to 0$ the axes z^s and z^b coincide, and Φ, Ψ cannot be defined uniquely. To avoid this problem, one may choose of switch the axes x^s, y^s, z^s whenever Θ for a molecule is

approaching 0. A much more elegant remedy is provided by the singularity-free *quaternion* algorithm of Evans [Evans and Murad (1977)]. In this algorithm, four dependent trigonometric functions of the Euler angles are used in place of the three angles themselves to describe rotational motion.

10.4.4 Constraint dynamics

For molecules with internal torsional degrees of freedom (*e.g.*, alkanes) formulating the equations of motion in generalized coordinates becomes quite laborious. As already mentioned, there is an alternative approach, namely to formulate and carry out the MD simulation in cartesian coordinates, while at the same time accounting for the holonomic (*e.g.* bond length) constraints in the system.

Constraint dynamics algorithms are general and versatile. They are applicable to rigid linear and nonlinear polyatomic molecules, as well as to flexible (hinged) polyatomics. Furthermore, they can be used to constrain parts of a molecule selected at will without much effort.

As already mentioned, a bond length constraint between two sites amounts to an equation of the form

$$|\mathbf{r}_1 - \mathbf{r}_2|^2 = {d_{12}}^2$$

When bond-angle constraints are used, it is most convenient to represent them as pseudo-bond length constraints. For example [Figure 10.21(*a*)] to simulate water as a rigid polyatomic using the cartesian coordinates of its three sites, one must constrain the values of the two O-H bonds and the H-O-H bond angle. Instead of constraining the

bond angle, it is more convenient to constrain the distance H-H, effectively introducing a "pseudobond" whose length is kept fixed. The number of degrees of freedom of the molecule can be found as

$$3 \times 3 \text{ or } 9 \text{ cartesian coordinates } - 3 \text{ bond length constraints} = 6$$

as expected (3 translational and 3 overall rotational degrees of freedom). Methane, on the other hand, can be simulated as a rigid polyatomic in cartesian coordinates using 4 bond and 5 pseudobond constraints. The net number of degrees of freedom is again $15 - 9 = 6$, as expected [Figure 10.21(b)]. In the case of a butane molecule in the united atom representation with fixed bond lengths and bond angles one can use three bond and two pseudobond constraints, resulting in a total of $12 - 5 = 7$ degrees of freedom (three translational, three rotational, and one torsional) [see Figure 10.21 (c)]. Through such "triangulation" it is possible to constrain any bonded geometry one wishes.

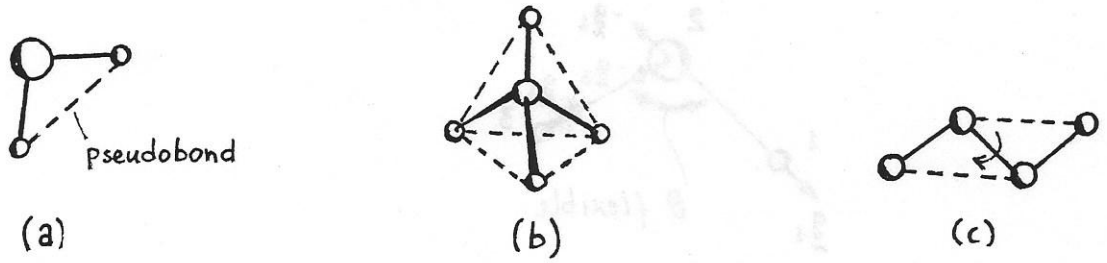

Figure 10.21 Introduction of pseudobonds ("triangulation") to constrain bond angles in model molecules. (a) water; (b) methane; (c) butane in a united atom representation

As one can readily deduce from a constraint Lagrangian formulation, each length constraint gives rise to a force acting along the bond or pseudobond. The constraint forces appear in the equations of motion for the cartesian coordinates of the sites; their magnitude is always such as to prevent distortion of the molecular shape.

As a simple example of how constraint dynamics is formulated, consider a water model with fixed bond lengths but a flexible bond angle. Energetic consequences of distortions in the bond angle θ are incorporated in the potential energy function of the system. Let the three sites in a molecule be numbered as shown in Figure 10.22. We will use the symbol $\mathbf{g}_1$ to denote the force on site 1 due to the bond 12, whose length is constrained, and $\mathbf{g}_3$ to denote the force on site 3 due to the constrained bond 23. The direction of forces $\mathbf{g}_1$ and $\mathbf{g}_3$ coincides with the direction of bonds 12 and 23, respectively, but their magnitude has to be calculated while tracking the motion of the sites. Site 2 will be subject to constraint forces $-\mathbf{g}_1$ and $-\mathbf{g}_3$, which can be viewed as reactions of the forces on 1 and 3, respectively.

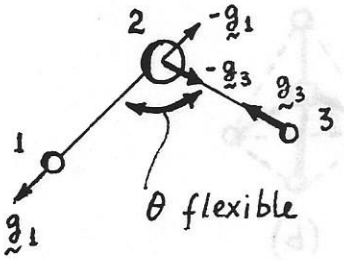

Figure 10.22 Constraint forces acting on the sites of a model water molecule with fixed bond lengths but a flexible bond angle.

A full constraint dynamics description of the motion of sites in the water molecule is given by the equations:

$$m_1 \ddot{\mathbf{r}}_1 = \mathbf{F}_1 + \mathbf{g}_1 \tag{10.89a}$$

$$m_3 \ddot{\mathbf{r}}_3 = \mathbf{F}_3 + \mathbf{g}_3 \tag{10.89b}$$

$$m_2 \ddot{\mathbf{r}}_2 = \mathbf{F}_2 - \mathbf{g}_1 - \mathbf{g}_3 \tag{10.89c}$$

$$\mathbf{g}_1 = \lambda_{12} (\mathbf{r}_1 - \mathbf{r}_2) \tag{10.90a}$$

$$\mathbf{g}_3 = \lambda_{23} (\mathbf{r}_3 - \mathbf{r}_2) \tag{10.90b}$$

$$\chi_{12}(\mathbf{r}_1, \mathbf{r}_2) = (\mathbf{r}_1 - \mathbf{r}_2)^2 - d_{12}^2 = 0 \tag{10.91a}$$

$$\chi_{23}(\mathbf{r}_2, \mathbf{r}_3) = (\mathbf{r}_3 - \mathbf{r}_2)^2 - d_{23}^2 = 0 \tag{10.91b}$$

The forces $\mathbf{F}_i$ are the "systematic" forces on sites. They are derived from a potential function $\mathcal{V}(\mathbf{r}_1, \mathbf{r}_2, \mathbf{r}_3, \ldots)$ that incorporates all intermolecular site-site interactions as well as the intramolecular bond angle bending energy for all molecules. Eqs. (10.90) simply require that the constraint forces be directed along the bonds. The magnitude of the forces is controlled by the undetermined (Lagrange) multipliers λ_{12} and λ_{23}. Eqs. (10.91) are the equations expressing te two bond constraints. In all, Eqs. (10.89) to (10.91) constitute a system of 9 differential equations and 8 algebraic equations in 17

unknown functions of time: $\mathbf{r}_1(t)$, $\mathbf{r}_2(t)$, $\mathbf{r}_3(t)$, $\mathbf{g}_1(t)$, $\mathbf{g}_3(t)$, $\lambda_{12}(t)$, and $\lambda_{13}(t)$. The numerical algorithm for constraint dynamics must calculate the constraint forces in parallel with integrating the equations of motion governing the system trajectory.

A generic constraint dynamics algorithm. A general algorithm for solving the MD problem with constraints has been presented by Ryckaert, Ciccotti, and Berendsen (1977). The constraint MD problem is written, in general, as

$$m_i \ddot{\mathbf{r}}_i = \mathbf{F}_i + \mathbf{g}_i \tag{10.92}$$

$$\chi_{ij}(\mathbf{r}_i, \mathbf{r}_j) = \mathbf{r}_{ji}^2 - d_{ij}^2 \equiv (\mathbf{r}_i - \mathbf{r}_j)^2 - d_{ij}^2 = 0 \tag{10.93}$$

$$\mathbf{g}_i = \frac{1}{2} \sum_j \lambda_{ij} \nabla_{\mathbf{r}_i} \chi_{ij} = \sum_j \lambda_{ij} \mathbf{r}_{ji} \tag{10.94}$$

where $\mathbf{F}_i = -\nabla_{\mathbf{r}_i} \mathcal{V}$ the systematic force on site i, $\mathbf{g}_i$ the total constraint force on site i, and Eqs. (10.93) are the bond or pseudobond length constraint equations. Let n_c be the number of constraints of the type (10.93) and N be the total number of sites. Then we have a problem consisting of $3N$ differential and n_c algebraic equations in the $3N + n_c$ unknown functions $\mathbf{r}_i(t)$, $\lambda_{ij}(t)$. Ryckaert *et al*'s algorithm proceeds as follows:

- Use a Verlet scheme to advance Eq. (10.92) for the sites by one step, ignoring the constraint forces altogether:

$$\mathbf{r}_i'(t + \delta t) = 2\,\mathbf{r}(t) - \mathbf{r}(t - \delta t) + \frac{\delta t^2}{m_i} \mathbf{F}_i(t) \tag{10.95}$$

  If the positions $\mathbf{r}_i'$ were assigned to the sites, the molecule would be distorted.

- The *actual* positions of the sites, taking into account the constraint forces, will be [Verlet scheme on the complete Eq. (10.92)]:

$$\mathbf{r}_i(t+\delta t;\{\lambda_{ij}\}) = \mathbf{r}'_i(t+\delta t) + \frac{\delta t^2}{m_i}\,\mathbf{g}_i(t;\{\lambda_{ij}\}) = \mathbf{r}'_i(t+\delta t) - \frac{\delta t^2}{m_i}\sum_j \lambda_{ij}\,\mathbf{r}_{ij}(t) \quad (10.96)$$

where the λ_{ij} are yet undetermined.

- Substituting the above expressions for $\mathbf{r}_i(t+\delta t)$ into the constraint equations (10.93), one obtains

$$[\mathbf{r}_i(t+\delta t;\{\lambda_{ij}\}) - \mathbf{r}_j(t+\delta t;\{\lambda_{ij}\}]^2 - d_{ij}^2 = 0 \quad (10.97)$$

Eqs. (10.97) constitute a set of *quadratic* algebraic equations in the unknowns $\{\lambda_{ij}\}$. The solution to this system must be obtained iteratively. If the Newton-Raphson method is used, then a $n_c \times n_c$ system of linear algebraic equations must be solved at each iteration.

- Once the $\{\lambda_{ij}\}$ have been determined, their substitution into Eq. (10.96) gives the actual atomic postions at time $t+\delta t$. The MD integration step has been completed.

The SHAKE and RATTLE algorithms. The SHAKE constraint dynamics algorithm (Ryckaert *et al.*, 1977) avoids the numerical solution of the quadratic $n_c \times n_c$ system of equations in $\{\lambda_{ij}\}$, Eq.(10.97), which is quite memory- and compute-intensive for large systems. Instead, the algorithm goes through the constraint equations one by one, cyclically, adjusting the site coordinates so as to satisfy each equation in turn. Clearly, whenever a site is involved in more than one constraints, it is impossible to ensure that all of them will be satisfied in one pass. The procedure of going through all constraints is

repeated, until all constraints are satisfied with prescribed tolerance. The algorithm is very popular in commercial simulation packages; the iterative procedure it employs can be quite inefficient, however, especially in the presence of bond angle constraints. An improvement of the SHAKE algorithm known as RATTLE was proposed by Andersen (1983). RATTLE employs the velocity version of the Verlet algorithm to integrate the dynamical equations.

The algorithm of Edberg, Evans, and Morris. This interesting algorithm [Edberg, Evans, and Morris (1986)] reduces the computations required for determining the constraint forces $\{\lambda_{ij}\}$ by substituting a *linear* system of equations in $\{\lambda_{ij}\}$ in place of the quadratic system, Eq. (10.97). These linear equations are formulated by considering the second time derivatives of the constraint equations (10.93):

$$\mathbf{r}_{ji}^2 - d_{ij}^2 = 0 \Rightarrow 2\mathbf{r}_{ji} \cdot \dot{\mathbf{r}}_{ji} = 0 \Rightarrow \mathbf{r}_{ji} \cdot \ddot{\mathbf{r}}_{ji} + (\dot{\mathbf{r}}_{ji})^2 = 0 \tag{10.98}$$

One then solves the following system of algebraic and differential equations simultaneously:

$$m_i \ddot{\mathbf{r}}_i = \mathbf{F}_i + \mathbf{g}_i \tag{10.92}$$

$$\mathbf{g}_i = \sum_j \lambda_{ij} \mathbf{r}_{ji} \tag{10.94}$$

$$\mathbf{r}_{ji} \cdot \ddot{\mathbf{r}}_{ji} + (\dot{\mathbf{r}}_{ji})^2 = 0 \tag{10.98}$$

Note that site velocities enter this formulation explicitly. Upon substitution of the site accelerations from Eq. (10.92) into Eq. (10.98), one obtains a linear system in $\{\lambda_{ij}\}$; the determination of the $\{\lambda_{ij}\}$, therefore, reduces to the solution of a linear matrix equation

at each step. Standard predictor-corrector or velocity Verlet methods are usable for integrating Eq. (10.92). It is remarkable that the bond lengths d_{ij} do not appear in the Edberg, Evans, and Morris scheme. One relies upon the second derivative equations (10.98) to preserve the geometry of the molecule. In practice, the molecular shape is gradually distorted as numerical error accumulates. Whenever this distortion exceeds a prescribed limit, the correct molecular geometry is restored by minimizing the functions

$$\Phi = \sum_{ij} \left(\mathbf{r}_{ij}^2 - d_{ij}^2\right)^2 \text{ (bond penalty function)} \tag{10.99}$$

$$\Psi = \sum_{ij} \left(\mathbf{r}_{ij} \cdot \dot{\mathbf{r}}_{ij}\right)^2 \text{ (velocity penalty function)} \tag{10.100}$$

Constraint dynamics of linear and planar polyatomic molecules. In trying to formulate constraint dynamics approaches for linear or planar polyatomic molecules in cartesian coordinates, one encounters a difficulty in identifying the appropriate number of linearly independent constraints. In the case of the linear triatomic CO_2, for example [Figure 10.23 (a)] constraint MD in $3 \times 3 = 9$ cartesian coordinates should employ $9 - 5 = 4$ constraints. Costraining the two C - O and the O-O distances is straightforward; how the fourth constraint should be introduced is not apparent, however. A similar situation arises with a planar molecule of more than three sites, such as the united atom benzene of Fig 10.23(a). In this case, $18-6 = 12$ constraints are needed. While one can write 12 bond and pseudobond constraints by trangulating the molecule as shown in Figure 10.23(a), one discovers that the resulting constraint matrix is singular, because all bonds and pseudobonds lie on the same plane. A solution for this problem has been proposed by Ciccotti, Ferrario, and Ryckaert (1982). One tracks the dynamics not for

all sites, but for a basic subset of "primary" sites for which the constraint problem is well- posed. The rest of the sites ("secondary" sites) transfer the systematic and inertial forces exerted on them onto the primary sites via the bonds. In this approach, CO_2 would be represented as two primary sites and one secondary site, while benzene would be represented as three primary sites and three secondary sites [see Figure 10.23(b)].

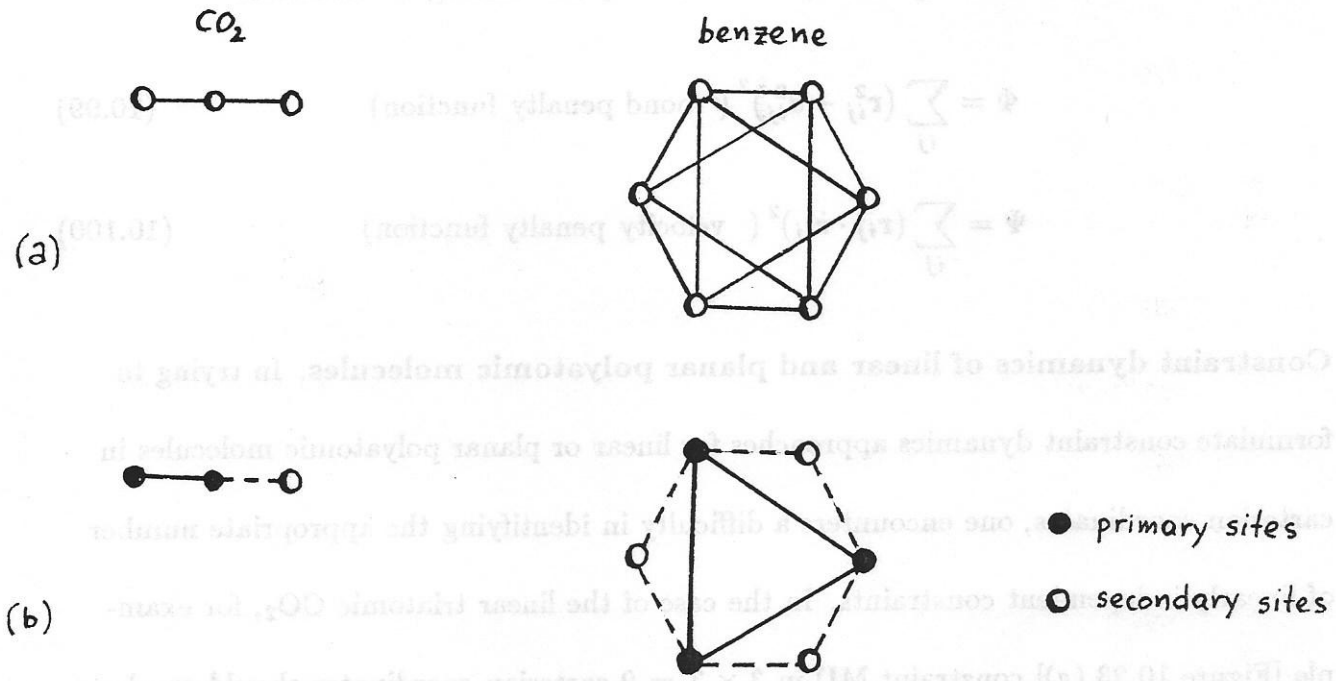

Figure 10.23 (a) A linear triatomic (CO_2) and a planar polyatomic molecule (benzene). (b) The motion of these molecules can be tracked with constraint dynamics by defining a set of primary sites, shown here as the black spheres. Secondary sites follow the motion of the primary sites while transmitting forces on them through the bonds.

10.4.5 General guidelines on the choice of MD algorithms

We summarize here some recommendations based on the preceding discussion of MD algorithms.

For simple fluid (monatomic) systems or for molecular systems where all bonded contributions are incorporated explicitly in the potential energy function, the Verlet velocity algorithm provides a good combination of simplicity and accuracy.

For rigid polyatomic systems one may choose to deal with the dynamics either in generalized coordinates or in cartesian coordinates with constraints. In the former case, the quaternion method with a Verlet leap-frog scheme for integrating the equations of motion gives good results. In the latter case the Edberg-Evans and Morris algorithm is satisfactory. In systems of linear or planar polyatomic molecules the MD must be performed on a rigid core of "primary" atoms as discussed in section 10.4.4.

For flexible polyatomic systems, the use of constraint methods with cartesian coordinates of sites is advantageous over the use of generalized coordinates. Both the Edberg-Evans Morris and the RATTLE algorithm can be used with satisfactory results. It is advisable to constrain bonds but not bond angles; constraining the bond angles affects the dynamics of conformational isomerization while leading to very modest increases in efficiency. The development of simulation algorithms is still a very active area, and the researcher should be constantly aware of new developments in the field.

10.4.6 Molecular dynamics in ensembles other than the microcanonical

Conventional MD is carried out on a model systems formed from a primary box of constant dimensions and consisting of interaction sites that move subject to interactions among themselves. As already pointed out in section 10.4.1, the resulting simulation, upon equilibration, samples the $NVE\mathbf{P}$ ensemble. The temperature at the simulated thermodynamic state can be estimated as a time average (ergodic hypothesis) of an "instantaneous" temperature $\mathcal{T}$ that reflects the total kinetic energy of the model system.

$$T = \langle \mathcal{T} \rangle \tag{10.101}$$

The phase function T is calculated from the kinetic energy $\mathcal{K}$ as

$$\mathcal{T} = \frac{2\mathcal{K}}{(3N - n_c)\, k_B} = \frac{1}{(3N - n_c)\, k_B} \sum_{i=1}^{N} \frac{|\mathbf{p}_i|^2}{m_i} \tag{10.102}$$

where N is the total number of atoms in the system, each of mass m_i and momentum $\mathbf{p}_i$, and n_c the total number of constraints. In counting n_c, one includes the total number of internal (geometric) constraints among the sites of the constituent molecules in the molecular model employed (*e.g.*, fixed bond lengths and bond angles); one also counts global constraints imposed on the system as a whole (*e.g.*, total momentum fixed at zero). In a conventional $NVE\mathbf{P}$ MD simulation of a simple fluid with $\mathbf{P} = \mathbf{0}$, for example, one must use Eq. (10.102) with $n_c = 3$ to calculate the instantaneous temperature from the total kinetic energy; even though no geometrical constraints are imposed on the molecules, the three components of the total momentum are constrained.

The thermodynamic pressure P is conveniently calculated from the virial theorem as an ensemble average of an "instantaneous pressure" $\mathcal{P}$:

$$P = \langle \mathcal{P} \rangle \tag{10.103a}$$

$$\mathcal{P} \equiv \rho k_B \mathcal{T} + \frac{1}{V} \mathcal{W}^{int} = \rho k_B \mathcal{T} + \frac{1}{3V} \sum_i \sum_{j>i} (\mathbf{r}_i - \mathbf{r}_j) \cdot \mathbf{F}_{ij} \tag{10.103b}$$

Note that the double summation form, Eq. (4.64), of the virial theorem has to be used here. Use of the single summation form, Eq. (4.63), is *wrong* in a system with periodic boundary conditions.

Useful thermodynamic quantities can be obtained from fluctuation relations. For example, the heat capacity C_v at constant volume can be obtained from

$$\langle \mathcal{V}^2 \rangle = \langle \mathcal{K}^2 \rangle = \frac{3}{2} N k_B^2 T^2 \left(1 - \frac{3 N k_B}{2 C_v} \right) \tag{10.104}$$

Since 1980, there has been much interest in designing MD methods that sample ensembles other than NVE. One can distinguish several categories of techniques for performing non-NVE MD. First, there are *heuristic*, or *ad hoc* methods. For example, a simple way to impose constant temperature in a MD simulation is to introduce "stochastic collisions" that rescale site velocities by preserving the direction of the velocity vector but picking a new magnitude for it from a Maxwell-Boltzmann distribution corresponding to a prescribed temperature; clearly, if the time between stochastic collisions experienced by a molecule is shorter than or commensurate with the correlation time of the velocity vector (see below) such a strategy will perturb the dynamics of the system. Secondly,

constraint methods can be used. For example, Evans et al. have imposed the requirement of constant temperature through introducing the nonholonomic constraint

$$\sum_i m_i \dot{\mathbf{r}}_i^2 = \frac{3}{2} N k_B T$$

in a non-Hamiltonian formulation based on the principle of least constraint of Gauss. Thirdly, there are *extended system*, or *extended ensemble* methods, which rest on the principles of Lagrangian dynamics.

Here we will only present a brief discussion of *extended ensemble* MD methods for the MD simulation of a system under a set of macroscopic constraints other than N, V, E.

The basic idea in an extended ensemble method is to introduce one or more *additional degrees of freedom* (along with the microscopic degrees of freedom), which correspond to one or more macroscopic quantities. Physically, each additional degree of freedom represents a "bath" or "reservoir" with which the original molecular system can interact.

Associated with each new degree of freedom are a "coordinate", a "velocity" (rate of change with time), and a "mass' (inertia).

A *kinetic energy* and a *potential energy* are assigned to each such degree of freedom. These energies are functions of the coordinates, velocities, and inertial variables mentioned above.

The *Lagrangian* of the extended system is written as a difference between kinetic and

potential energies that incoporate contributions both from the original (molecular) degrees of freedom and from the new degrees of freedom (reservoir).

The equations of motion for all degrees of freedom (molecular *and* reservoir) are derived from the Lagrangian using Eq. (10.57). In general, the equation of motion for the molecular degrees of freedom will be *different* from the Newtonian equations of motion describing the time evolution of the system in NVE dynamics.

The equations of motion of the extended system are integrated with one of the methods discussed in the previous sections.

If the potential energy and kinetic energy expressions for the additional (bath) degrees of freedom have been chosen appropriately, the steady-state probability density distribution in the phase space of the original (molecular) system, as generated by the extended system dynamics, will conform to the desired ensemble.

As follows from our general discussion of Lagrangian dynamics, there is an extended system Hamiltonian, derivable from the Lagrangian, which is conserved by the dynamics. This extended Hamiltonian contains contributions from the bath degrees of freedom and *no longer* corresponds to the total energy of the original molecular system.

As examples for the implementation of extended ensemble methods we will consider Nosé's method for MD in the canonical ensemble and Andersen's method for MD in the NPH (constant pressure and enthalpy) ensemble.

An extended system method for MD in the NVT ensemble. Nosé (1984) devised a method for performing dynamics under the macroscopic constraints of constant

system volume (or spatial extent) and temperature, which samples the phase-space probability density of the canonical ensemble.

An extra degree of freedom, s, is introduced that allows for energy to flow dynamically between the molecular system under study and a "heat reservoir" and thereby change the kinetic energy of the system. The reservoir temperature (set point) T_{eq} is an input parameter to the simulation. A "thermal inertia" (mass) Q is also introduced, which controls the frequency of fluctuations in the extra degree of freedom s.
The degree of freedom s is introduced as a scaling factor for particle velocities:

$$\mathbf{v} = s\,\dot{\mathbf{r}} \tag{10.105}$$

where $\mathbf{v}$ are the actual velocities of particles, defined with respect to real time, and $\dot{\mathbf{r}}$ the derivatives of position vectors with respect to simulation time. In other words, a "simulation time clock" is introduced in addition to the real time clock. Simulation time may be expanded or contracted relative to real time, and s enters as a scaling factor in this relationship:

$$(\text{realtimestep}) = (\text{simulation time step})\frac{1}{s}$$

s is a function of real time, *i.e.* what real time interval corresponds to a simulation time interval may change in the course of the simulation. Dots over symbols will denote derivatives with respect to simulation time. The potential energy contribution assigned to the extra degree of freedom s is

$$\mathcal{V}_s = (f+1)\,k_B\,T_{eq}\,\ln s \tag{10.106}$$

where f stands for the number of the original molecular system. For a system of N independent sites with periodic boundary conditions, $f = 3N - 3$, as explained above.

The kinetic energy contribution assigned to s is written as

$$\mathcal{K}_s = \frac{1}{2} Q \dot{s}^2 \tag{10.107}$$

Te Lagrangian of the extended system is

$$\mathcal{L}' = \mathcal{K}' - \mathcal{V}' = \mathcal{K} + \mathcal{K}_s - \mathcal{V} - \mathcal{V}_s =$$

$$\frac{1}{2} \sum_{i=1}^{N} m_i \, s^2 \, \dot{\mathbf{r}}_i^2 + \frac{1}{2} Q \dot{s}^2 - \mathcal{V}(\mathbf{r}) - (f+1) \, k_B \, T_{eq} \, \ln s$$

where the unprimed and primed quantities refer to the extended and original systems, respectively.

The vector of generalized coordinates $\mathbf{q}$ is the column vector

$$\mathbf{q} = \begin{bmatrix} \mathbf{r}_1 \\ \mathbf{r}_2 \\ \vdots \\ \mathbf{r}_N \\ s \end{bmatrix}$$

The equations of motion are derived from Eq. (10.57):

$$\frac{d}{dt} \left(\frac{\partial \mathcal{L}'}{\partial \dot{q}_k} \right) - \frac{\partial \mathcal{L}'}{\partial q_k} = 0$$

applied for $k = 1, 2, \ldots, 3N + 1$. They can be written as follows:

$$\ddot{\mathbf{r}}_i = \frac{\mathbf{F}_i}{m_i \, s^2} - 2 \, \frac{\dot{s} \, \dot{\mathbf{r}}_i}{s} \tag{10.108a}$$

$$Q \, \ddot{s} = \sum_{i=1}^{N} m_i \, s \, \dot{\mathbf{r}}_i^2 - (f+1) \, \frac{k_B}{s} \, T_{eq} \tag{10.108b}$$

Note the evolution equation (10.108b) for the extra degree of freedom s. Eqs. (10.108) are integrable, *e.g.* via a Gear predictor-corrector scheme.

The generalized momenta of the extended system are defined through Eqs. (3.1)

$$\mathbf{p}'_i = \frac{\partial \mathcal{L}'}{\partial \dot{\mathbf{r}}_i} = m_i s^2 \dot{\mathbf{r}}_i \quad (i = 1, 2, \ldots, 3N) \tag{10.109a}$$

$$p'_s = \frac{\partial \mathcal{L}'}{\partial \dot{s}} = Q \dot{s} \tag{10.109b}$$

A *conserved quantity* of the dynamics will be the extended system Hamiltonian

$$\mathcal{H}'(\mathbf{p}', \mathbf{q}') = \sum_k \dot{q}_k p'_k - \mathcal{L}(\mathbf{q}, \dot{\mathbf{q}}) =$$

$$\frac{1}{2} \sum_i m_i s^2 \dot{\mathbf{r}}_i^2 + \frac{1}{2} Q \dot{s}^2 + \mathcal{V}(\mathbf{r}) + (f+1) k_b T_{eq} \ln s \tag{10.110}$$

$\mathcal{H}'$ is a constant of the simulation, which we will denote with E'.

Nosé (1984) presents a proof that the partition function of the extended system corresponding to the Hamiltonian of Eq. (10.110) is

$$Q_{NVE'} = \frac{1}{(f+1)\,h} \left(\frac{2\pi Q}{k_B T_{eq}} \right)^{1/2} \exp\left(\frac{E'}{k_B T_{eq}} \right) \times$$

$$\frac{1}{N!\,h^f} \int d^{3N}p \int d^{3N}r \exp\left[-\mathcal{H}(\mathbf{p}, \mathbf{r}) \frac{1}{k_B T_{eq}} \right] \tag{10.111}$$

where

$$\mathbf{p}_i = \frac{\mathbf{p}'_i}{s} = m_i s \dot{\mathbf{r}}_i = m_i \mathbf{v}_i \text{ the } \textit{actual} \text{ momentum vector of site } i \tag{10.112}$$

The first three factors of $Q_{NVE'}$ have to do with the bath degree of freedom, while the rest is immediately recognizable as the phase-space probability distribution of the original system. Clearly, the distribution over the phase space $(\mathbf{r}, \mathbf{p})$ of the original system

defined by Eq. (10.111) obeys the canonical ensemble, as desired. Therefore, for any function $\mathcal{A}$ of the atomic coordinates and momenta

$$\left\langle \mathcal{A}\left(\frac{\mathbf{p}'}{s}, \mathbf{r}\right)\right\rangle' = \langle \mathcal{A}(\mathbf{p}, \mathbf{r})\rangle_{NVT} \tag{10.113}$$

where thhe primed angular brackets indicate averaging over the extended ensemble MD, whereas the unprimed brackets indicate equilibrium averaging over the canonical ensemble phase-space distribution of the original system at temperature T_{eq}. In particular, for the instantaneous temperature

$$\mathcal{T} = \frac{2}{f\,k_B}\sum_{i=1}^{N}\frac{\mathbf{p}_i'^2}{2\,m_i\,s^2} = \frac{2}{f\,k_B}\sum_{i=1}^{N}\frac{m_i}{2}\mathbf{v}_i^2 \tag{10.114}$$

one has

$$\text{Average}\quad \langle \mathcal{T}\rangle' = T_{eq} \tag{10.115a}$$

$$\text{Variance}\quad \left\langle (\delta\mathcal{T})^2\right\rangle' = \left\langle (\mathcal{T} - T_{eq})^2\right\rangle = T_{eq}^2\frac{2}{f} \tag{10.115b}$$

Note that the instantaneous temperature does fluctuate about the set point, but the fluctuations are weak for a system with a large number of degrees of freedom.

The real time duration of a Nosé simulation is obtained by multiplying the total simulation time by $\langle s^{-1}\rangle'$. For a well-designed simulation, this factor should be around unity.

The choice of the inertial factor Q affects the system dynamics. If $Q \to \infty$ (large thermal inertia), one obtains very slow energy transfer between the molecular system and the reservoir, and the dynamics approach those of a constant energy (NVE) system. On the other hand, if Q becomes very small, then the dynamical behavior is significantly distorted by the frequent energy exchange with the bath; this is especially true

of slow, collective motions. A "reasonable" choice of Q should yield dynamical characteristics (*e.g.*, time correlation functions, self- diffusivities) coincident with those obtained through NVE simulation at the same thermodynamic state. That such a "reasonable" choice of Q is possible has been established empirically. The magnitude of Q affects the frequency of oscillations of the bath variable s. The period of oscillations in s can be estimated as $t_0 = 2\pi \left(\frac{Q \langle s^2 \rangle}{2 f k_B T_{eq}} \right)^{1/2}$. If this period is smaller than the correlation time of a dynamical process, the dynamics of that process may be distorted by the extended-ensemble method. For NVT-MD simulations of simple liquids, Nosé recommends a choice of Q that leads to $t_0 \simeq 1$ps.

Hoover (1985) modified Nosé's constant temperature technique, arriving at an equilvalent set of dynamical equations that are free of time scaling. (*i.e.*, there is no need to distinguish between simulation time and real time, which is convenient). The resulting scheme is often referred to as the "Nosé-Hoover thermostat".

An extended system method for MD in the NPH ensemble. As a second example of extended ensemble methods we consider the constant pressure-constant enthalpy MD introduced in a pioneering paper by H.C. Andersen (1980). Here the extra degree of freedom is the box volume V. The simulation box is "pulsating", as if its walls were a piston exposed to a constant pressure reservoir. Again, there is an inertial parameter W resisting changes in the volume, which is often referred to as the "piston mass". The set value of pressure is denoted as P_{eq}.

As in isothermal-isobaric MC, scaled molecular positions and velocities are introduced:

$$\mathbf{r} = V^{1/3} \mathbf{s} \qquad (10.116a)$$

$$\mathbf{v} = V^{1/3}\,\dot{\mathbf{s}} \tag{10.116b}$$

The potential and kinetic energy associated with the extra degree of freedom are

$$\mathcal{V}_V = P_{eq}\,V \tag{10.117a}$$

$$\mathcal{K}_V = \frac{1}{2}\,W\,\dot{V}^2 \tag{10.117b}$$

The Lagrangian formulation for the extended system leads to the equations of motion

$$\ddot{\mathbf{s}}_i = \frac{1}{m_i\,V^{1/3}}\,\mathbf{F}_i - \frac{2}{3}\dot{\mathbf{s}}_i\,\frac{\dot{V}}{V} \tag{10.118a}$$

$$\ddot{V} = (\mathcal{P} - P_{eq}) \tag{10.118b}$$

where

$$\mathcal{P} = \frac{1}{3\,V}\left(\sum_i m_i\,\mathbf{v}^2 + \sum_i \sum_{i<j} (\mathbf{r}_i - \mathbf{r}_j)\cdot\mathbf{F}_{ij}\right) \tag{10.119}$$

A conserved quantity is the Hamiltonian of the extended system,

$$\mathcal{H}' = V^{2/3}\sum_{i=1}^{N}\frac{m_i\,\dot{\mathbf{s}}_i^2}{2} + \mathcal{V}\left(V^{1/3}\mathbf{s}_1,\ldots,V^{1/3}\mathbf{s}_N\right) + \frac{1}{2}W\,\dot{V}^2 + P_{eq}\,V \tag{10.120}$$

Andersen gives a rigorous proof that the equilibrium distribution of phase space points of the original system generated by the extended system dynamics corresponds to an NPH ensemble, with instantaneous enthalpy kept constant at

$$H = \mathcal{H}' - \frac{1}{2}\,W\left\langle\dot{V}^2\right\rangle' = \mathcal{H}' - \frac{1}{2}\,k_B\left\langle\mathcal{T}\right\rangle'$$

The value of the inertial factor W affects the dynamics. Large W lead to slow volume fluctuations; in the limit $W \to \infty$ one recovers NVE dynamics. Small W, on the other

hand, lead to fast volume fluctuations that may distort dynamical processes in the system. Andersen recommends choosing W so that the period of volume fluctuations is roughly equal to the time for a sound wave to traverse the simulation box.

Other developments

A variety of extended ensemble MD approaches have been developed in recent years. We briefly mention some of them below.

Parrinello and Rahman (1980, 1981) presented an extension of the Andersen method that allows fluctuations in the *shape* of the simulation box and permits studying a system under conditions of constant number of particles, *stress tensor*, and enthalpy ($N\tau H$ MD). The method is valuable in studying phase transformations in solids, wherein the symmetry of the crystal lattice may change (*e.g.*, orthorhombic to monoclinic); such transformations would be disallowed in a cubic simulation box.

A constant temperature and pressure (NPT) or constant temperature and stress ($N\tau T$) extended ensemble MD method that is based on a combination of the Nosé and Andersen or Parrinello-Rahman techniques has been described by Nosé (1984).

Nosé and Klein (1983) have carried over the constant temperature and constant pressure extended ensemble methods to molecular systems.

Extended ensemble MD techniques using a variable number of particles, and therefore capable of sampling the probability density of the grand canonical ensemble, have been developed recently [Cagin and Pettitt (1991)].

Perhaps most interesting is the *ab initio* MD technique of Car and Parrinello (1985). In this technique, electronic degrees of freedom are incorporated into the extended ensemble

simulation. The method tracks the motion of nuclear coordinates and at the same time determines the energy of interaction through *ab initio* quantum mechanical density functional theory of the inomogeneous electron gas surrounding the nuclei (see Chapter 11). No inputs about the potential energy hypersurface are required; the quantum mechanics of the system is solved "on the fly" along with the molecular dynamics. Although very taxing on computer time, this *ab initio* MD technique has been applied to systems such as Si and GaAs melts and liquid H_2O with excellent results.

10.5 Structure from molecular simulations

10.5.1 Information stored in tape file

Information about the structure, thermodynamic and dynamic properties of the system under investigation is extracted by post-processing the results generated from long molecular simulation runs. The results are typically stored in binary form in a large "tape file".

In the case of *Monte Carlo*, the tape file contains information about the configurations visited during the run. Site coordinates $\mathbf{r}_i$, orientation angles Φ_i, Θ_i, Ψ_i and torsion angles ϕ_i may be stored for all molecules. In variable volume simulations, the box dimensions must be stored. In addition, the system potential energy $\mathcal{V}$ and virial $\mathcal{W}$ (for the calculation of pressure) may be stored. This information is stored every 5^{th} or 10^{th} MC cycle, a cycle being a sequence of N attempted moves. More frequent storage would

increase the size of the tape file without contributing much independent information, as successive steps are highly correlated.

In the case of *molecular dynamics*, one stores the time t, the system configuration ($\mathbf{r}_i, \Phi_i, \Theta_i, \Psi_i$, ϕ_i, bath degrees of freedom employed in extended ensemble methods) as well as momentum space variables (atomic or molecular center of mass velocities $\mathbf{v}_i$, molecular angular velocities ω_i, *etc.*). The parent image coordinates of molecules (prior to imposition of periodic boundary conditions) may be stored to facilitate monitoring diffusional motion, although these can be regenerated from the primary box image positions without much trouble [Allen and Tildesley (1987)]. In addition, the forces $\mathbf{F}_i$, torques $\mathcal{T}_i$, total energy E, potential energy $\mathcal{V}$, kinetic energy associated with site translation, center of mass translation, and rotation, amd the virial $\mathcal{W}$ are typically stored. This information is stored evey 5^{th} or 10^{th} integration time step.

Block average analysis can be used to determine the degree of correlation between stored configurations and thereby estimate the statistical error in ensemble averaged quantities obtained from the simulation. For a discussion of block averaging methods and statistical inefficiency, see Allen and Tildesley (1987), p. 192.

10.5.2 Accumulation of pair distribution functions

The pair distribution function $g(r)$ is a valuable piece of structural information one can obtain from molecular simulations; it is related to thermodynamic properties and testable against experimental information about structure from diffraction. From the

discussion of section 9.1.1 [Eq. (9.16) and Figure 9.1] it is apparent that the pair distribution in an isotropic system is obtainable as

$$g(r) = \frac{\rho(r)}{\rho} \tag{10.121}$$

where $\rho(r)$ the local density of particles within a spherical shell of radius r to $r + dr$ centered at a site and averaged over all configurations of the system, and ρ the mean (macroscopic) density of sites. Extensions of this approach to systems consisting of more than one type of particles have been discussed in chapter 9.

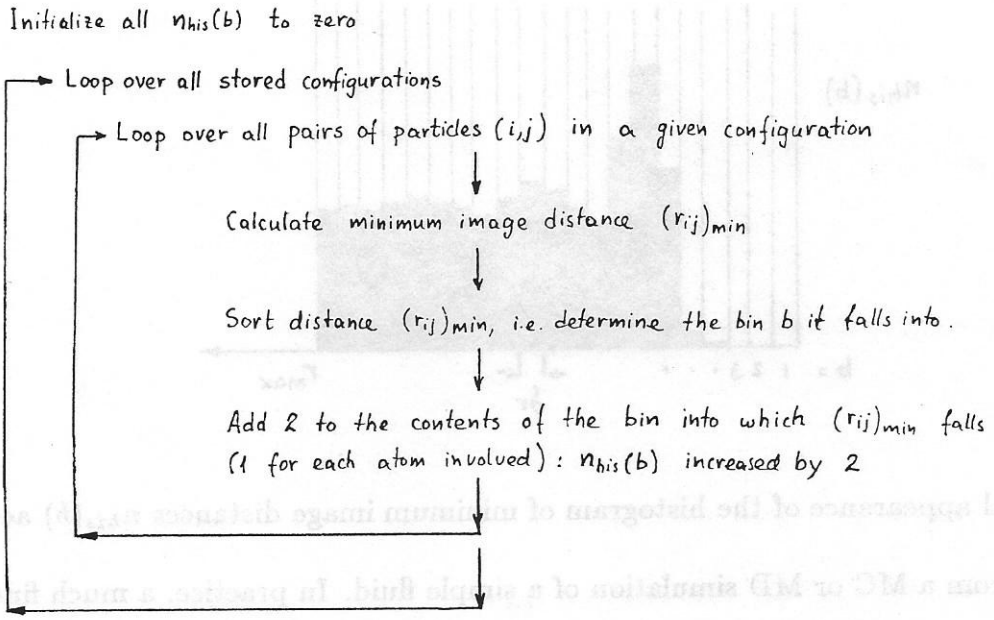

Figure 10.24 Loop over all configurations and all pairs of particles used to accumulate a histogram $n_{his}(b)$ of the minimum image pair distances from the stored results of a MC or MD simulation.

The procedure for calculating $g(r)$ from a simulation starts by analyzing all stored configurations to determine the distances between all *minimum image pairs*. It is only minimum image pairs that contribute independent structural information; the spatial

correlation between no-minimum image pairs may be strongly affected by the artificial periodicity of the model system, as is obvious for pairs of different images of the same site. Having identified all minimum image pairs, one can calculate $g(r)$ trough the following expression, suggested by Eq. (10.121):

$$g(r) = \frac{\text{Number of particles at distance } r \text{ to } r+dr \text{ from a central particle}}{\text{Number of particles at distance } r \text{ to } r+dr \text{ from a central particle in an ideal gas system of the same density}} \qquad (10.122)$$

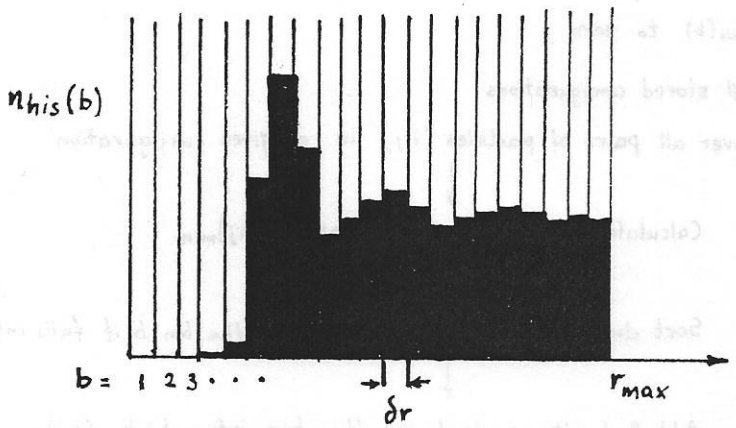

Figure 10.25 General appearance of the histogram of minimum image distances $n_{his}(b)$ accumulated from a MC or MD simulation of a simple fluid. In practice, a much finer resolution δr is used along the distance axis.

To compute the numerator and denominator of Eq. (10.122), the r-axis between 0 and a certain value r_{max} (beyond which structure is expected to have washed out) is subdivided into bins of width δr. Let b be the index of the bin between r and $r+\delta r$. Let $n(b)$ and $n^{id}(b)$ be the numerator and denominator, respectively, of Eq. (10.122) corresponding to bin b. One accumulates a histogram $n_{his}(b)$ of numbers of minimum image

pairs by looping over all stored configurations and all pairs of particles in each configuration, as shown in Figure 10.24. The general appearance of this histogram for a simple fluid simulation is shown schematically in Figure 10.25.

The numerator in Eq. (10.122) is formed from the histogram $n_{his}(b)$ accumulated as described above through

$$n(b) = \frac{n_{his}(b)}{N\,\tau_{run}} \tag{10.123}$$

where N is the total number of particles in the model system and τ_{run} the total number of [equilibrated] configurations analyzed.

The denominator of Eq. (10.122) is calculated by straightforward geometric arguments. If $r_{max} \leq L/2$, where L the edge length of the simulation box, one can use

$$n^{id}(b) = \frac{4\pi\rho}{3}\left[(r+\delta r)^3 - r^3\right] \tag{10.124}$$

Structural information can be obtained up to the maximum value of the minumum image distance, which, for cubic model systems, equals the half-diagonal of the simulation box. (*i.e.*, $r_{\max}$ can be as high as $L\,3^{1/2}/2$). For separations higher than $L/2$, Eq. (10.124) has to be modified, as the minimum image locus that corresponds to distances r to $r+\delta r$ is no longer spherical. A procedure that can be followed in this case is described in Theodorou and Suter (1985b).

The pair distribution function is obtained from the histogram quantities $n(b)$ and $n^{id}(b)$ by

$$g\left(r+\frac{1}{2}\delta r\right) = \frac{n(b)}{n^{id}(b)} \tag{10.125}$$

(assignment to the middle of each bin).

The above procedure is readily adapted for the calculation of site-site distribution functions $g^{\alpha\beta}$ for all pairs of sites (α, β) in a molecular system. Procedures for the calculation of X-ray and neutron diffraction patterns from $g^{\alpha\beta}(r)$ have been discussed in section 9.1.4.

10.5.3 Quantifying molecular orientation

In many applications (*e.g.*, interfaces, polymers, liquid crystals) it is important that one quantify the orientation of molecules or of characteristic structural elements (*e.g.*, bonds, dipole moments) with respect to a fixed coordinate frame or with respect to each other. Let $\mathbf{u}_i$ be a unit vector characterizing the orientation of the structural element of interest; for example, $\mathbf{u}_i$ may be a principal axis or a bond vector or the end-to-end vector of a molecule. Let the angle between the unit vectors embedded in two molecules i and j be θ_{ij} (see Figure 10.26). The second order Legendre polynomial

$$P_2(\cos\theta_{ij}) = \frac{1}{2}\left[3\,(\mathbf{u}_i \cdot \mathbf{u}_j)^2 - 1\right] \tag{10.126}$$

when ensemble averaged, provides information on relative orientational tendencies of the molecules. In practice, one often accumulates the quantity ("order parameter")

$$\langle P_2(\cos\theta_{ij})\rangle_{|\mathbf{r}_i - \mathbf{r}_j| = r} = \frac{1}{2}\left[3\left\langle (\mathbf{u}_i \cdot \mathbf{u}_j)^2 \right\rangle_{|\mathbf{r}_i - \mathbf{r}_j| = r} - 1\right] \tag{10.127}$$

as a function of the distance r.

A value of the order parameter close to 1 indicates strong tendency towards parallel orientation. A value close to $-1/2$ betrays a trend towards perpendicular orientation, while complete absence of orientational correlation results in an order parameter of 0.

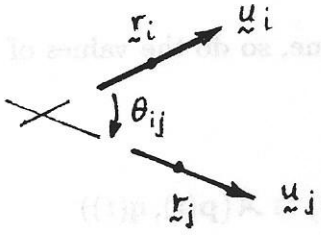

Figure 10.26 For the definition of an order parameter describing the relative orientation of two molecules.

10.6 Dynamical information from equilibrium MD

10.6.1 Time correlation functions

In this section we briefly discuss how information about the characteristic times of dynamical processes and about transport coefficients can be extracted from equilibrium MD simulations. As already pointed out, MD simulation is a valuable source for such information, especially concerning phenomena with short characteristic times.

Consider a system at equilibrium under given external constraints. The probability distribution of the system in phase space will conform to an equilibrium ensemble, with

density $\rho^{eq}(\mathbf{X}) \equiv \rho^{eq}(\mathbf{p},\mathbf{q})$ [compare section 3.2.3]. Let

$$\mathcal{A}(\mathbf{X}) = \mathcal{A}(\mathbf{p},\mathbf{q}) \tag{10.127a}$$

$$\mathcal{B}(\mathbf{X}) = \mathcal{B}(\mathbf{p},\mathbf{q}) \tag{10.127b}$$

be two functions of the phase-space representative point (microstate) of the system. As the microscopic state changes with time, so do the values of $\mathcal{A}$ and $\mathcal{B}$. We will use the notation

$$\mathcal{A}(t) \equiv \mathcal{A}\left(\mathbf{p}(t),\mathbf{q}(t)\right) \tag{10.128a}$$

$$\mathcal{B}(t) \equiv \mathcal{B}\left(\mathbf{p}(t),\mathbf{q}(t)\right) \tag{10.128b}$$

Furthermore, we will use the symbolism $\delta\mathcal{A}(t)$, $\delta\mathcal{B}(t)$ to denote the deviations between the instantaneous values of $\mathcal{A}$ and $\mathcal{B}$ along a dynamical trajectory and the corresponding ensemble average values:

$$\delta\mathcal{A}(t) \equiv \mathcal{A}(t) - \langle\mathcal{A}(t)\rangle = \mathcal{A}(t) - \langle\mathcal{A}\rangle \tag{10.129a}$$

$$\delta\mathcal{B}(t) \equiv \mathcal{B}(t) - \langle\mathcal{B}(t)\rangle = \mathcal{B}(t) - \langle\mathcal{B}\rangle \tag{10.129b}$$

We define the *non-normalized time correlation function* between $\mathcal{A}$ and $\mathcal{B}$ as

$$C_{\mathcal{AB}}(t) \equiv \langle\delta\mathcal{A}(t_1)\,\delta\mathcal{B}(t_1+t)\rangle = \langle[\mathcal{A}(t_1) - \langle\mathcal{A}\rangle]\,[\mathcal{B}(t_1+t) - \langle\mathcal{B}\rangle]\rangle \tag{10.130}$$

For a system at equilibrium, the ensemble average on the right-hand side of Eq. (10.130) will not depend on the time origin t_1, but only on the time separation t. Also, by the

ergodic hypothesis, the ensemble averages in Eq. (10.130) can be substituted by time averages over all time origins t_1.

$$C_{\mathcal{AB}}(t) = C_{\mathcal{AB}}(-t) = \langle \delta\mathcal{A}(0)\, \delta\mathcal{B}(t) \rangle = \langle \delta\mathcal{A}(t)\, \delta\mathcal{B}(0) \rangle \tag{10.131}$$

In this discussion we will restrict our attention to the case where $\mathcal{A}$ and $\mathcal{B}$ are the same quantity. We will call

$$C_{\mathcal{AA}} = \langle \delta\mathcal{A}(t_1)\, \delta\mathcal{A}(t_1 + t) \rangle = \langle \delta\mathcal{A}(0)\, \delta\mathcal{B}(t) \rangle \tag{10.132}$$

the *non-normalized (time) autocorrelation function* of $\mathcal{A}$.

We define the *normalized autocorrelation function* of $\mathcal{A}$ as

$$c_{\mathcal{AA}}(t) = \frac{C_{\mathcal{AA}}(t)}{C_{\mathcal{AA}}(0)} = \frac{\langle \delta\mathcal{A}(t)\, \delta\mathcal{A}(0) \rangle}{\left\langle (\delta\mathcal{A})^2 \right\rangle} \tag{10.133}$$

The denominator in Eq, (10.133) is a measure of the fluctuation in $\mathcal{A}$ at thermodynamic equilibrium.

$c_{\mathcal{AA}}$ assumes a value of 1 for $t = 0$ (perfect correlation at the time origin). As t elapses, $c_{\mathcal{AA}}$ decays, ultimately approaching 0 as $t \rightarrow \infty$. Physically, $c_{\mathcal{AA}}$ measures how the property $\mathcal{A}$ *loses memory of its initial value* as a result of molecular motion in the system. A characteristic time, over which this memory persists, can be defined as

$$\tau_{\mathcal{A}} = \int_0^\infty c_{\mathcal{AA}}(t)\, dt \tag{10.134}$$

$\tau_{\mathcal{A}}$ is the *correlation time* of $\mathcal{A}$. For some (but not all!) dynamical processes, the autocorrelation function $c_{\mathcal{AA}}$ is found to decay exponentially with time at long times (Figure

10.27). For such processes, an estimate of τ_A can be obtained from the long-time slope of the autocorrelation function in semilogarithmic coordinates.

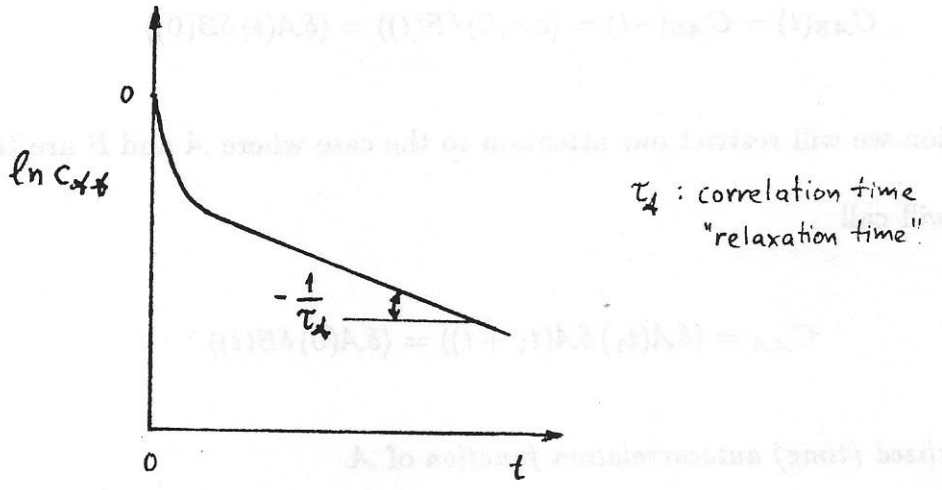

Figure 10.27 Schematic of an autocorrelation function that decays exponentially at long times.

Autocorrelation functions are of great significance, because

- they provide a picture of molecular motion in a material system
- the time integrals τ_A of flux autocorrelation functions are related to macroscopic transport coefficients.
- the Fourier transforms $\hat{c}_{AA}(\omega)$ are often related to experimentally obtainable spectra.

As an example, consider the velocity autocorrelation function in a fluid. The non-normalized autocorrelation function for the α-component of the molecular velocity is

$$C_{v_\alpha v_\alpha}(t) = \langle v_{C\alpha}(t)\, v_{i\alpha}(0)\rangle = \frac{1}{N}\left\langle \sum_i v_{i\alpha}(t)\, v_{i\alpha}(0)\right\rangle \qquad (10.135)$$

where it is recognized that $\delta v_{i\alpha} \equiv v_{i\alpha}$, as $\langle v_{i\alpha} \rangle = 0$, and that the average for a given molecule i will equal the average over all molecules. The expression on the right hand side of Eq. (10.135) (average over all molecules) has distinct advantages in simulations, as it drastically increases the sample size over which the autocorrelation function is accumulated.

The non-normalized autocorrelation function for the velocity vector $\mathbf{v}$ is

$$C_{\mathbf{vv}}(t) = \langle \mathbf{v}_i(t)\, \mathbf{v}_i(0) \rangle = \frac{1}{N} \left\langle \sum_i \mathbf{v}_i(t)\, \mathbf{v}_i(0) \right\rangle = C_{v_x\, v_x}(t) + C_{v_y\, v_y}(t) + C_{v_z\, v_z}(t) \quad (10.136)$$

and the normalized velocity autocorrelation function is

$$c_{\mathbf{vv}}(t) = \frac{C_{\mathbf{vv}}(t)}{C_{\mathbf{vv}}(0)} = \frac{C_{\mathbf{vv}}(t)}{\frac{3\, k_B\, T}{m}} = \frac{m}{3\, k_B\, T} \langle \mathbf{v}_i(t) \cdot \mathbf{v}_i(0) \rangle \quad (10.137)$$

The Fourier transform of the non-normalized velocity autocorrelation function is

$$\hat{C}_{\mathbf{vv}}(\omega) = \int_{-\infty}^{\infty} C_{\mathbf{vv}}(t)\, e^{-i\,\omega\, t}\, dt = 2 \int_0^{\infty} C_{\mathbf{vv}}(t)\, \cos \omega t\, dt \quad (10.138)$$

The general behavior of the functions $c_{\mathbf{vv}}(t)$ and $\hat{C}_{\mathbf{vv}}(\omega)$ for liquid argon at its triple point is shown in Figure 10.28. At this liquid density, the decay of $c_{\mathbf{vv}}$ with time is pronouncedly nonexponential. The velocity autocorrelation function passes to negative values and asymptotically approaches zero at long times from below. The change in sign reflects the reversal in the direction of motion as a molecule collides with the "cage" of other molecules that surround it in the dense liquid. The "long time tail" follows a scaling law of the form $|c_{\mathbf{vv}}| \propto t^{-3/2}$. This slow decay is caused by collective hydrodynamic effects (moving molecule creates a "wake" of other molecules with which it interacts).

Note the relatively short correlation time for molecular velocities (practically all correlation has subsided at ca. 1.5ps). The general appearance of the Fourier transform $\hat{C}_{vv}(\omega)$ is shown in Fig. 10.28(b). Such spectra are experimentally measurable through dynamic neutron scattering.

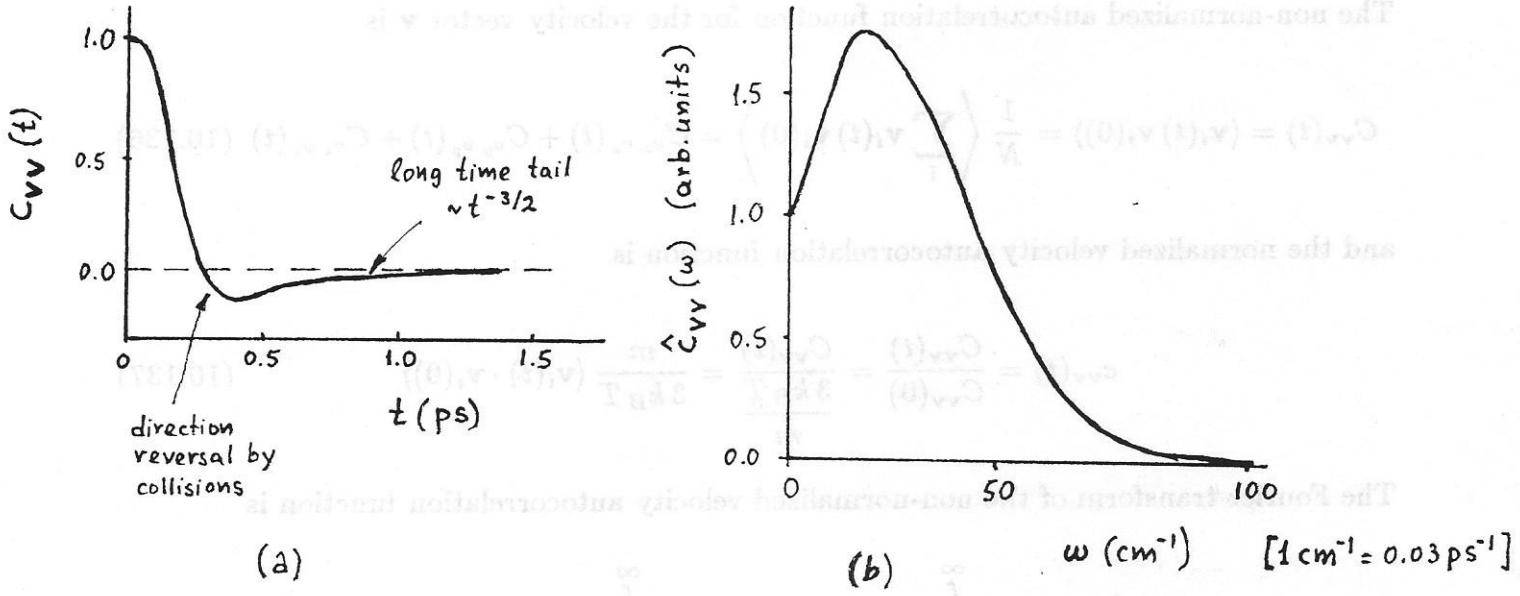

Figure 10.28 (a) Velocity autocorrelation function and (b) its Fourier transform for liquid argon at its triple point.

As mentioned above, the time integrals of autocorrelation functions are related to *transport coefficients*. As we know from chemical engineering, transport coefficients describe the response (flux) that is elicited in a system by the imposition of a perturbation (driving force) that causes the system to *depart from equilibrium*. Autocorrelation functions, on the other hand, describe the rate at which *spontaneous fluctuations* created

within a system *at equilibrium* die out with time. A very important connection between equilibrium correlation functions and transport coefficients is established by *linear response theory* [Hansen and McDonald (1986)]. We will not go into the linear response formalism here. The basic idea is that, if a system is kept away from equilibrium by a *small* driving force, then the rate at which it will approach equilibrium when the driving force is removed (transport phenomenon) will equal the rate at which a spontaneous fluctuation arising in the absence of a driving force will disappear (autocorrelation function). Consider, for example, the binary diffusivity D. This transport coefficient is defined as a proportionality constant between the flux (molecules per unit area per unit time) of either species in a binary system relative to the system center of mass, and the concentration gradient. For concentration gradients that are not too steep on a molecular length scale, such a linear (Fickian) relationship between flux and driving force is satisfactory. If one observes the binary system *at equilibrium* (system macroscopically homogeneous) at the molecular level, one is likely to see fluctuations wherein the flux of the two species is not strictly zero (equilibrium average value), but, say, there is an excess of type 1 molecules moving to the right and an excess of tyle 2 molecules moving to the left. Such a fluctuation creates a small microscopic flux or current, which will eventually die out as the motion of molecules is randomized through collisions. Linear response theory connects the rate at which this microscopic interdiffusion current will die out at equilibrium with the interdiffusion coefficient. A prominent role in linear response theory is played by autocorrelation functions of the form $\left\langle \dot{A}(t)\, \dot{A}(0) \right\rangle$. These appear in

relations of the form

$$\gamma = \int_0^\infty dt \left\langle \dot{\mathcal{A}}(t)\, \dot{\mathcal{A}}(0) \right\rangle = \int_0^\infty dt\, C_{\dot{\mathcal{A}}\dot{\mathcal{A}}}(t) \tag{10.139}$$

where γ a transport coefficient, within a multiplicative constant. Relations of the type of Eq. (10.139) are known as *Green-Kubo* relations.

An example is provided by the Green-Kubo relation for the *self-diffusivity*. The self-diffusivity in the x-direction is related to the time integral of the autocorrelation function for the x-component of the molecular velocity, defined in Eq. (10.135):

$$D_{s,xx} = \int_0^\infty dt\, \langle \dot{x}_i(t)\, \dot{x}_i(0) \rangle = \int_0^\infty dt\, \langle v_{ix}(t)\, v_{ix}(0) \rangle \tag{10.140}$$

while the orientationally averaged self-diffusivity (trace of the self- diffusivity tensor) is

$$D_s = \frac{1}{3} \int_0^\infty dt\, \langle \dot{\mathbf{r}}_i(t)\, \dot{\mathbf{r}}_i(0) \rangle = \frac{1}{3} \int_0^\infty dt\, \langle \mathbf{v}_i(t)\, \mathbf{v}_i(0) \rangle =$$

$$\frac{1}{3} \int_0^\infty dt \left\langle \frac{1}{N} \sum_{i=1}^{N} \mathbf{v}_i(t)\, \mathbf{v}_i(0) \right\rangle = \frac{1}{3} \left(D_{s,xx} + D_{s,yy} + D_{s,zz} \right) \tag{10.141}$$

Mathematically equivalent to the Green-Kubo expression, Eq. (10.139), is the *Einstein* relation

$$2\gamma\, t = \left\langle \left[\mathcal{A}(t) - \mathcal{A}(0) \right]^2 \right\rangle \quad (\text{for } t >> t_{\dot{\mathcal{A}}}\text{, long times}) \tag{10.142}$$

For example, the Einstein relations for the self-diffusivities $D_{s,xx}$ and D_s are

$$2\, D_{s,xx}\, t = \left\langle \left[x_i(t) - x_i(0) \right]^2 \right\rangle \text{, or } D_{s,xx} = \lim_{t \to \infty} \frac{\left\langle \left[x_i(t) - x_i(0) \right]^2 \right\rangle}{2\, t} \tag{10.143}$$

$$2\, D_s\, t = \frac{1}{3} \left\langle \left[\mathbf{r}_i(t) - \mathbf{r}_i(0) \right]^2 \right\rangle \text{, or } D_s = \lim_{t \to \infty} \frac{\left\langle \left[\mathbf{r}_i(t) - \mathbf{r}_i(0) \right]^2 \right\rangle}{6\, t} \tag{10.144}$$

Again, in applying Eq. (10.144) to MD simulations, it is advantageous to perform an average over all particles:

$$D_s = \lim_{t\to\infty} \frac{\left\langle \frac{1}{N}\sum_i [\mathbf{r}_i(t) - \mathbf{r}_i(0)]^2 \right\rangle}{6\,t} \tag{10.145}$$

More important for engineering applications is the *interdiffusion (binary diffusion) coefficient* D. A Green-Kubo relation for this quantity is

$$D = \frac{1}{3\,N}\left(\frac{\partial^2 (\beta\, G/N)}{\partial x_1^2}\right)_{P,T} \int_0^\infty \langle \mathbf{j}^c(t)\cdot\mathbf{j}^c(0)\rangle \; dt \tag{10.146}$$

where $\mathbf{j}^c(t)$ is the *microscopic interdiffusion current*, defined as

$$\mathbf{j}^c(t) = x_2\,\mathbf{j}^1(t) - x_1\,\mathbf{j}^2(t) \tag{10.147}$$

with

$$\mathbf{j}^\nu(t) = \sum_{i=1}^{N_\nu} \mathbf{u}_i(t) \tag{10.148}$$

$\mathbf{j}^\nu$, $(\nu = 1,2)$ equals the number of molecules of species ν times the velocity of the center of mass of the swarm of molecules of species ν. Thus, $\mathbf{j}^c$ is a flux of the two species relative to each other. N is the total number of molecules in the system, $x_\nu = N_\nu/N$ is the mole fraction of species ν, and G the total Gibbs energy function. Observe that D consists of a thermodynamic factor and a mobility factor. The mobility factor is a time integral of a flux autocorrelation function, as discussed above.

The *shear viscosity* can be obtained from the following Green-Kubo relation:

$$\eta = \frac{V}{k_B\,T}\int_0^\infty dt\; \langle \mathcal{P}_{\alpha\beta}(t)\,\mathcal{P}_{\alpha\beta}(0)\rangle\,, \quad \alpha \neq \beta \tag{10.148}$$

where $\mathcal{P}_{\alpha\beta}$ is a nondiagonal component of the instantaneous pressure tensor (*i.e.*, the opposite of an instantaneous shear stress, compare virial theorem):

$$\mathcal{P}_{\alpha\beta} = \frac{1}{V}\left(\sum_i \frac{p_{i\alpha}\, p_{i\beta}}{m_i} + \sum_i r_{i\alpha} F_{i\beta}\right) \tag{10.149}$$

The corresponding Einstein relation for the shear viscosity is

$$2\,t\,\eta = \frac{V}{k_B\,T}\left\langle \left[\mathcal{G}_{\alpha\beta}(t) - \mathcal{G}_{\alpha\beta}(0)\right]^2 \right\rangle \tag{10.150}$$

with

$$\mathcal{G}_{\alpha\beta} = \frac{1}{V}\sum_i r_{i\alpha}\, p_{i\beta} \tag{10.151}$$

Care must be exercised in applying these relations to model systems with periodic boundary conditions.

The *thermal conductivity* λ_T is obtainable in a similar way from the time autocorrelation function of the energy current:

$$\lambda_T = \frac{V}{k_B\,T^2}\int_0^\infty dt\ \langle j_\alpha^\epsilon(t)\, j_\alpha^\epsilon(0)\rangle \tag{10.152}$$

where

$$j_\alpha^\epsilon = \frac{d}{dt}\left\{\frac{1}{V}\sum_i r_{i\alpha}\left(\epsilon_i - \langle\epsilon_i\rangle\right)\right\} \tag{10.153}$$

is a component of the energy current, with

$$\epsilon_i = \frac{\mathbf{p}_i^2}{2\,m_i} + \frac{1}{2}\sum_{j\neq i}\mathcal{V}_{pair}(r_{ij}) \tag{10.154}$$

The corresponding Einstein relation is

$$2\,t\,\lambda_T = \frac{V}{k_B\,T^2}\left\langle\left[\delta\epsilon_\alpha(t) - \delta\epsilon_\alpha(0)\right]\right\rangle \tag{10.155}$$

$$\delta\epsilon_\alpha = \frac{1}{V}\sum_i r_{i\alpha}\,(\epsilon_i - \langle\epsilon_i\rangle) \qquad (10.156)$$

In general, the estimation of transport coefficients is more reliable if based on the Einstein, as opposed to the Green-Kubo route; this is because the Green-Kubo approach calls for integrating the long-time tails of correlation functions, and the error in accumulating these tails from a MD simulation of short duration may be significant. As opposed to D_s, the properties D, η, λ_T are *collective* properties of the system and not properties of individual particles. In estimating them from Green-Kubo or Einstein relations, one cannot average over all particles, as was done in Eqs. (10.141) and (10.145). Consequently, these collective transport coefficients require much more computer time than the self-diffusivity in order to be estimated reliably; this problem is partly alleviated by use of non-equilibrium molecular dynamics simulations. [Allen and Tildesley (1987)].

10.6.2 Calculation of autocorrelation functions from MD trajectories

In accumulating an autocorrelation function $C_{\mathcal{A}\mathcal{A}}(t)$ from the tape file of an equilibrium MD simulation, the ensemble average appearing in the definition of $C_{\mathcal{A}\mathcal{A}}$ is substituted by a time average. Multiple time origins τ_0 along the MD trajectory are used to obtain the time average [see Figure 10.29(a)]. Let τ be a counter for time, such that $t = \tau\,\delta t$ with δt the time interval between configurations stored on tape. Then,

$$C_{\mathcal{A}\mathcal{A}}(\tau) = \langle \mathcal{A}(\tau)\,\mathcal{A}(0)\rangle = \frac{1}{\tau_{max}}\sum_{\tau_0=1}^{\tau_{max}} \mathcal{A}(\tau_0)\,\mathcal{A}(\tau_0+\tau) \qquad (10.156)$$

Clearly, the maximal of time origins used in (10.156) has to satisfy

$$\tau_{max} \leq \tau_{run} - \tau \qquad (10.157)$$

where τ_{run} the overall duration of the run in units of δt. Short-time correlations are obtainable with greater precision than long-time correlations. The sample size becomes very limited at τ values commensurate with τ_{run}. Therefore, to safely estimate the entire $C_{\mathcal{A}\mathcal{A}}(t)$, the length of the simulation must be significantly larger than the correlation time $\tau_{\mathcal{A}}$ associated with the property $\mathcal{A}$. $C_{\mathcal{A}\mathcal{A}}$ values are typically accumulated in parallel for all τ, $0 \leq \tau \leq \tau_{cor}$, through a double loop over all stored data [see Figure 10.29(b)]. Some memory-saving techniques for performing this calculation are discussed by Allen and Tildesley (1987).

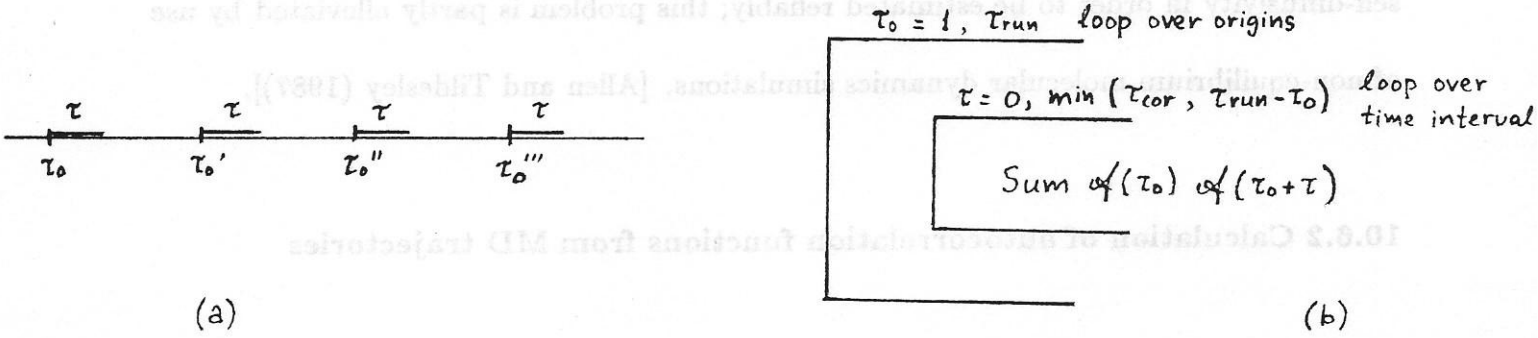

Figure 10.29 (a) Schematic showing how the value of a time correlation function at τ is calculated from a MD run using multiple time origins. (b) Double loop over all origins and all time intervals used in accumulating the time correlation function.

When the accumulation of autocorrelation functions up to $\tau_{max} \simeq \tau_{run}$ is required, the computations associated with the double loop of Figure 10.29(b) become

excessive. A computationally more expedient method is to accumulate $C_{\mathcal{A}\mathcal{A}}(t)$ via two fast Fourier transforms, by invoking the correlation theorem of Fourier analysis. First, the $\mathcal{A}(t)$ obtained from the run is transformed using FFT to obtain $\hat{\mathcal{A}}(\omega)$; this involves $\tau_{run} \log_2 \tau_{run}$ operations. Next the Fourier transform of the autocorrelation function is obtained from $\hat{\mathcal{A}}(\omega)$ as

$$\hat{C}_{\mathcal{A}\mathcal{A}}(\omega) = \frac{1}{\tau_{max}} \hat{\mathcal{A}}^*(\omega)\, \hat{\mathcal{A}}(\omega)$$

Finally, $\hat{C}_{\mathcal{A}\mathcal{A}}(\omega)$ is back transformed via FFT to obtain $C_{\mathcal{A}\mathcal{A}}(t)$.

10.7 General organization of a simulation code

We close this section with a very brief reference to the structure of a molecular simulation code. The code must be designed so that minimal information is lost in the event of a computer crash, and so that it can be restarted with minimal difficulty.

Input/Output

File manipulations should be kept to the minimum. Usually, three types of output files are accumulated:

- *Output file.* This contains information about the model system size, potential parameters used, conditions simulated, overall run duration, number of equilibration steps used, and other information needed for fully identifying the run and reproducing it, if necessary. Instantaneous quantities $(\mathcal{V}, E, \mathcal{T}, \mathcal{P}, \ldots)$ are written at frequent intervals so as to allow one to inspect the progress of the run. Accumulated simulation averages are printed out at the end.

- *Configuration file.* In this file, the configuration and momenta (for MD), seed for random number generation (for MC) and accumulators of average properties are saved periodically, so as to allow restart in the event of a crash. Old information is overwritten; *i.e.*, the file contains the most recent snapshot of instantaneous and averaged information available. It is also known as the "crash file".
- *Tape file.* In this file, all positions, velocities, accelerations, energies, *etc.* are stored at frequent intervals, as discussed in section 10.5.1. New information is appended, *i.e.*, the file contains a detailed record of the entire simulation. The simulation results are obtained by post-processing this file. This file is typically extremely large and is written in as economic a form (from the point of view of storage) as possible; it need only be machine readable (by the postprocessing program).

Program Structure

The general flow of computations is as follows [Allen and Tildesley (1987)]:

- Read/print simulation parameters and general information about the run.
- Set up auxiliary parameters. Initialize potential tables and neighbor lists.
- Read in the starting configuration file.
- Initialize property accumulators for the calculation of averages.
- Position the tape file at the right point for output.
- calculate/print energy, forces, and other important characteristics of the initial configuration.
- Main body of the simulation (loop over steps)

- Move particles

- Update running averages

- Print out instantaneous properties and current averages on output file (one every IPRINT steps)

- Print out detailed information on the tape file (once every ITAPE steps)

- Save current configuration on the crash file (once every ISAVE steps)

· Accumulate and print final averages, fluctuation quantities, statistics on the run.

· Close all files and exit.

References

Adams, D.J. (1974). Chemical potential of hard sphere fluids by Monte Carlo methods. *Mol. Phys.* **28**, 1241-1252.

Allen, M.P. and Tidesley, D.J. (1987). *Computer Simulation of Liquids.* Clarendon press, Oxford.

Andersen, H.C. (1980). Molecular dynamics simulations at constant pressure and/or temperature *J. Chem. Phys.* **72**, 2384-2393.

Andersen, H.C. (1983). Rattle: a 'velocity' version of the shake algorithm for molecular dynamics calculations *J. Comput. Phys.* **52**, 24-34.

Cagin, T. and Pettitt, B.M. (1991). Molecular dynamics with a variable number of molecules *Mol. Phys.* **72**, 169-175.

Car, R., Parrinello, M. (1985). Unified approach for molecular dynamics and density functional theory *Phys. Rev. Lett.* **55**, 2471-2474.

Ciccotti, G., Ferrario, M., Ryckaert, J.P. (1982). Molecular dynamics of rigid systems in cartesian coordinates. A general formulation. *Mol. Phys.* **47**, 1253 - 1264.

Edberg, R., Evans, D.J., Morris, G.P. (1986). Constrained molecular dynamics: Simulations of liquid alkanes with a new algorithm. *J. Chem. Phys.* **84**, 6933 - 6939.

Evans, D.J. and Murad, S. (1977). Singularity-free algorithm for molecular dynamics simulation of rigid polyatomics. *J. Mol.Phys.* **34**, 327-331.

Flory, P.J. (1969). *Statistical mechanics of chain molecules.* Wiley, New York.

Gear, C.W. (1971). *Numerical initial value problems in ordinary differential equations.* Prentice-Hall, Englewood Cliffs.

Goldstein. H. (1980). *Classical mechanics*, 2nd Ed. Addison-Wesley, Reading.

Hansen, J.P., McDonald, I. (1986). *Theory of simple liquids*, 2nd Ed. Academic Press, London.

Hirschfelder, J.O., Curtiss, C.F., and Bird, R.B. (1954). *Molecular theory of gases and liquids.* Wiley, New York (1954).

Hockney R.W. (1970). The potential calculation and some applications. *Methods comput. Phys.* **9**, 136-211.

Hoover, W.G. (1985). Canonical dynamics: equilibrium phase-space distributions. *Phys. Rev. A* **31**, 1695-1697.

Jorgensen, W.L. (1981). Revised TIPS for simulations of liquid water and aqueous solutions. *J. Chem. Phys.* **77**, 4156-4163.

Kalos, M.H.; Whitlock, P.A. (1986). *Monte Carlo methods*, Vol. I: *Basics.* Wiley, New York.

Kemeny, J.G., Snell, J.L. (1960). *Finite Markov Chains.* van Nostrand, Princeton.

Knuth, D. (1973). *The art of computer programming.* (2nd edn). Addison- Wesley, Reading, MA.

Maitland, G.C., Rigby, M., Smith, E.B., Wakeham, W.A. (1981). *Intermolecular forces: their origin and determination.* Clarendon press, Oxford.

Maréchal, G., Ryckaert, J.P. (1983). Atomic vs. molecular description of transport properties in polyatomic fluids: n-butane as an example *Chem. Phys. Lett.* **101**, 548-554.

Matsuoka, O., Clementi, E., Yoshimine, M. (1976). CI study of the water dimer potential surface. *J. Chem. Phys.* **64**, 1351-1361.

Metropolis, N., Rosenbluth, A.W., Rosenbluth, M.N., Teller, A.H., Teller, E. (1953). Equation of state calculations for fast computing machines. *J. Chem. Phys.* **21**, 1087-1092.

Norman, G.E., Filinov. V.S. (1969). Investigations of phase transitions by a Monte Carlo method. *High Temp. (USSR)* **7**, 216-222.

Nosé, S. (1984). A molecular dynamics method for simulations in the canonical ensemble. *Mol. Phys.* **52**, 255-268.

Nosé, S., Klein, M.L. (1983). Constant pressure dynamics for molecular systems. *Mol. Phys.* **50**, 1055-1076.

Parrinello, M, Rahman, A. (1980). Crystal structure and pair potentials: a molecular dynamics study. *Phys. Rev. Lett.* **45**, 1196-1199.

Parrinello, M, Rahman, A. (1981). Polymorphic transitions in single crystals: a new molecular dynamics method *J. Appl. Phys.* **52**, 7182-7190.

Press, W.H., Flannery, B.P., Teukolsky, S.A., Vetterling, W.T. (1986). *Numerical recipes.* Cambridge University Press, Cambridge.

Ryckaert, J.P., Ciccotti, G., Berendsen, H.J.C. (1977). Numerical integration of the cartesian equations of motion of a system with constraints: molecular dynamics of n-alkanes. *J. Comput. Phys.* **23**, 327-341.

Swope, W.C., Andersen, H.C., Berens, P.H., Wilson, K.R. (1982). A computer simulation method for the calculation of equilibrium constants for the formation of physical clusters of molecules: application to small water clusters. *J. Chem. Phys.* **76**, 637-649.

Theodorou, D.N., Suter U.W. (1985a). Detailed molecular structure of a vinyl polymer glass. *Macromolecules* **18**, 1467-1478.

Theodorou, D.N., Suter U.W. (1985b). Geometrical considerations in model systems with periodic boundaries *J. Chem. Phys.* **82**, 955-966.

Van Gunsteren, W.F., Berendsen, H.J.C. (1977). Algorithms for macromolecular dynamics and constraint dynamics. *Mol. Phys. 34*, 1311-1327.

Verlet, L. (1967). Computer 'experiments' on classical fluids. I. Thermodynamical properties of Lennard-Jones molecules. *Phys. Rev.* **159**, 98-103.

Wood, W.W. (1968). Monte Carlo calculations for hard disks in the isothermal- isobaric ensemble. *J. Chem. Phys.* **48**, 415-434.